

Molecular Design Based on Artificial Neural Networks, Integer Programming and Grid Neighbor Search

Naveed Ahmed Azam¹, Jianshen Zhu¹, Kazuya Haraguchi¹, Liang Zhao², Hiroshi Nagamochi¹
and Tatsuya Akutsu³

¹ Department of Applied Mathematics and Physics, Kyoto University, Kyoto 606-8501, Japan

² Graduate School of Advanced Integrated Studies in Human Survavibility (Shishu-Kan), Kyoto University, Kyoto 606-8306, Japan

³ Bioinformatics Center, Institute for Chemical Research, Kyoto University, Uji 611-0011, Japan

Abstract

A novel framework has recently been proposed for designing the molecular structure of chemical compounds with a desired chemical property using both artificial neural networks and mixed integer linear programming. In the framework, a chemical graph with a target chemical value is inferred as a feasible solution of a mixed integer linear program that represents a prediction function and other requirements on the structure of graphs. In this paper, we propose a procedure for generating other feasible solutions of the mixed integer linear program by searching the neighbor of output chemical graph in a search space. The procedure is combined in the framework as a new building block. The results of our computational experiments suggest that the proposed method can generate an additional number of new chemical graphs with up to 50 non-hydrogen atoms.

Keywords: Machine Learning, Integer Programming, Cheminformatics, Materials Informatics, QSAR/QSPR, Molecular Design.

1 Introduction

Background Analysis of chemical compounds is one of the important applications of intelligent computing. Indeed, various machine learning methods have been applied to the prediction of chemical activities from their structural data, where such a problem is often referred to as *quantitative structure activity relationship* (QSAR) [1, 2]. Recently, neural networks and deep-learning technologies have extensively been applied to QSAR [3].

In addition to QSAR, extensive studies have been done on inverse quantitative structure activity relationship (inverse QSAR), which seeks for chemical structures having desired chemical activities under some constraints. Since it is difficult to directly handle chemical structures in both QSAR and inverse QSAR, chemical compounds are usually represented as vectors of real or integer numbers, which are often called *descriptors* in chemoinformatics and correspond to *feature vectors* in machine learning. One major approach in inverse QSAR is to infer feature vectors from given chemical activities and constraints and then reconstruct chemical structures from these feature vectors [4, 5, 6], where chemical structures are usually treated as undirected graphs. However, the reconstruction itself is a challenging task because the number of possible chemical graphs is huge. For example, chemical graphs with up to 30 atoms (vertices) C, N, O, and S may exceed 10^{60} [7].

Indeed, it is NP-hard to infer a chemical graph from a given feature vector except for some simple cases [8]. Due to this inherent difficulty, most existing methods for inverse QSAR do not guarantee optimal or exact solutions.

As a new approach, extensive studies have recently been done for inverse QSAR using *artificial neural networks* (ANNs), especially using graph convolutional networks [9]. For example, recurrent neural networks [11, 12], variational autoencoders [10], grammar variational autoencoders [13], generative adversarial networks [14], and invertible flow models [15, 16] have been applied. However, these methods do not yet guarantee optimal or exact solutions.

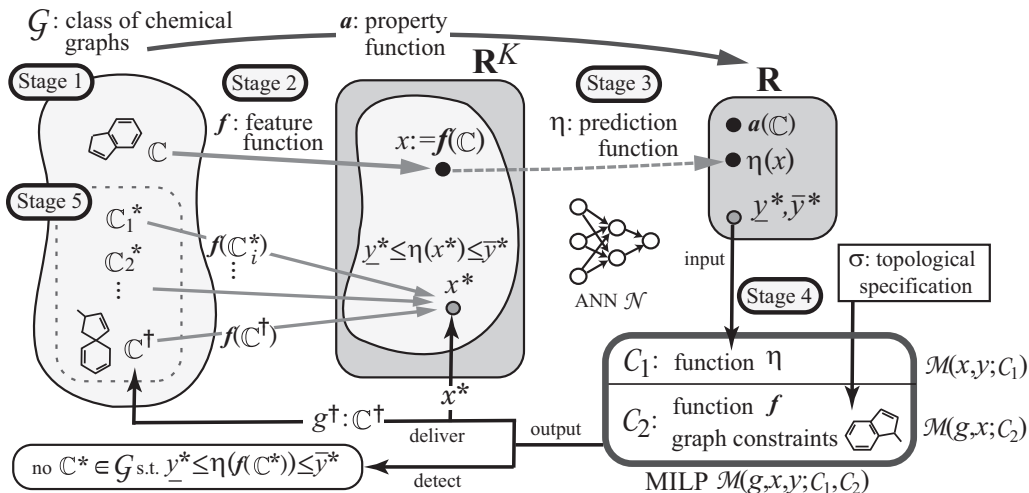


Figure 1: An illustration of a framework for inferring a set of chemical graphs \mathbb{C}^* .

Framework Akutsu and Nagamochi [17] proved that the computation process of a given ANN can be simulated with a mixed integer linear programming (MILP). Based on this, a novel framework for inferring chemical graphs has been developed and revised [18, 24], as illustrated in Figure 1. It constructs a prediction function in the first phase and infers a chemical graph in the second phase. The first phase of the framework consists of three stages. In Stage 1, we choose a chemical property π and a class \mathcal{G} of graphs, where a property function a is defined so that $a(\mathbb{C})$ is the value of π for a compound $\mathbb{C} \in \mathcal{G}$, and collect a data set D_π of chemical graphs in \mathcal{G} such that $a(\mathbb{C})$ is available for every $\mathbb{C} \in D_\pi$. In Stage 2, we introduce a feature function $f: \mathcal{G} \rightarrow \mathbb{R}^K$ for a positive integer K . In Stage 3, we construct a prediction function η with an ANN \mathcal{N} that, given a vector $x \in \mathbb{R}^K$, returns a value $y = \eta(x) \in \mathbb{R}$ so that $\eta(f(\mathbb{C}))$ serves as a predicted value to the real value $a(\mathbb{C})$ of π for each $\mathbb{C} \in D_\pi$. Given two reals \underline{y}^* and \bar{y}^* as an interval for a target chemical value, the second phase infers chemical graphs \mathbb{C}^* with $\underline{y}^* \leq \eta(f(\mathbb{C}^*)) \leq \bar{y}^*$ in the next two stages. We have obtained a feature function f and a prediction function η and call an additional constraint on the substructures of target chemical graphs a *topological specification*. In Stage 4, we prepare the following two MILP formulations:

- MILP $\mathcal{M}(x, y; \mathcal{C}_1)$ with a set \mathcal{C}_1 of linear constraints on variables x and y (and some other auxiliary variables) simulates the process of computing $y := \eta(x)$ from a vector x ; and
- MILP $\mathcal{M}(g, x; \mathcal{C}_2)$ with a set \mathcal{C}_2 of linear constraints on variable x and a variable vector g that represents a chemical graph \mathbb{C} (and some other auxiliary variables) simulates the process of

computing $x := f(\mathbb{C})$ from a chemical graph \mathbb{C} and chooses a chemical graph \mathbb{C} that satisfies the given topological specification σ .

Given an interval with boundaries $\underline{y}^*, \overline{y}^* \in \mathbb{R}$, we solve the combined MILP $\mathcal{M}(g, x, y; \mathcal{C}_1, \mathcal{C}_2)$ to find a feature vector $x^* \in \mathbb{R}^K$ and a chemical graph \mathbb{C}^\dagger with the specification σ such that $f(\mathbb{C}^\dagger) = x^*$ and $\underline{y}^* \leq \eta(x^*) \leq \overline{y}^*$ (where if the MILP instance is infeasible then this suggests that there does not exist such a desired chemical graph). In Stage 5, we generate other chemical graphs \mathbb{C}^* such that $\underline{y}^* \leq \eta(f(\mathbb{C}^*)) \leq \overline{y}^*$ based on the output chemical graph \mathbb{C}^\dagger .

MILP formulations required in Stage 4 have been designed for chemical compounds with cycle index at most 2 [20]. Afterwards, a modeling of chemical compounds together with an MILP formulation has been improved so that a chemical compound with any graph structure can be treated (see Shi et al. [22]). Not only ANNs but also other machine learning methods have been used to construct a prediction function η in Stage 3 recently. Tanaka et al. [23] (resp., Zhu et al. [24]) used a decision tree (resp., linear regression) to construct a prediction function η in Stage 3 in the framework and derived an MILP $\mathcal{M}(x, y; \mathcal{C}_1)$ that simulates the computation process of a decision tree (resp., linear regression).

Contribution In the current framework, a chemical graph \mathbb{C}^\dagger with a desired chemical property π in Stage 4 is constructed as a feasible solution of an MILP $\mathcal{M}(g, x, y; \mathcal{C}_1, \mathcal{C}_2)$ before we generate isomers \mathbb{C}^* of \mathbb{C}^\dagger by an algorithm such as the dynamic programming algorithm due to Azam et al. [19]. In this paper, we design a procedure of generating solutions of the same MILP as a new building block in Stage 4 of the framework of inferring chemical graphs. When a feasible solution \mathbb{C}^\dagger of the MILP is constructed in Stage 4, we try to find other feasible solutions \mathbb{C}^* of the same MILP by solving the MILP with additional p_{\max} linear constraints for some integer p_{\max} . For this, we first prepare arbitrary linear functions $\theta_p : \mathbb{R}^K \rightarrow \mathbb{R}, p \in [1, p_{\max}]$ and consider a neighbor of \mathbb{C}^\dagger defined by a set of chemical graphs \mathbb{C}^* that satisfy linear constraints $\delta_1 \leq |\theta_p(f(\mathbb{C}^*)) - \theta_p(f(\mathbb{C}^\dagger))| \leq \delta_2, p \in [1, p_{\max}]$ for small reals $\delta_2 > \delta_1 > 0$. By changing the reals δ_2 and δ_1 systematically, we can search for new solutions of the same MILP other than \mathbb{C}^\dagger . As a candidate for a function θ_p , we can use a linear prediction function $\eta_\tau : \mathbb{R}^K \rightarrow \mathbb{R}$ for a different chemical property τ such as a function η_τ that has been obtained by linear regression. With a linear prediction function $\theta_p = \eta_\tau$, we can search for other chemical graphs \mathbb{C}^* by specifying a predicted value of \mathbb{C}^* for the property τ .

We implemented the framework with the new building block based on the two-layered model and the feature function proposed by Zhu et al. [24]. We used the same MILP $\mathcal{M}(g, x; \mathcal{C}_2)$ formulation proposed by Zhu et al. [24] and omit the details in this paper. From the results of our computational experiments, we observe that the proposed method can generate an additional number of chemical graphs \mathbb{C}^* in Stage 4 with up to 50 non-hydrogen atoms.

The paper is organized as follows. Section 2 introduces some notions on graphs, a modeling of chemical compounds and a choice of descriptors. Section 3 reviews the two-layered model. Section 4 introduces a new method of generating solutions of an MILP in Stage 4. Section 5 reports the results on computational experiments conducted for 47 chemical properties such as biological half life and boiling point for monomers and characteristic ratio and refractive index for polymers. Section 6 makes some concluding remarks. Some technical details are given in Appendices: Appendix A for all descriptors in our feature function; Appendix B for a full description of a topo-

logical specification; and Appendix C for the detail of test instances used in our computational experiment for Stages 4 and 5.

2 Preliminary

This section introduces some notions and terminologies on graphs, modeling of chemical compounds and our choice of descriptors.

Let \mathbb{R} , \mathbb{R}_+ , \mathbb{Z} and \mathbb{Z}_+ denote the sets of reals, non-negative reals, integers and non-negative integers, respectively. For two integers a and b , let $[a, b]$ denote the set of integers i with $a \leq i \leq b$. For a vector $x \in \mathbb{R}^p$, the j -th entry of x is denoted by $x(j)$.

Graph Given a graph G , let $V(G)$ and $E(G)$ denote the sets of vertices and edges, respectively. For a subset $V' \subseteq V(G)$ (resp., $E' \subseteq E(G)$) of a graph G , let $G - V'$ (resp., $G - E'$) denote the graph obtained from G by removing the vertices in V' (resp., the edges in E'), where we remove all edges incident to a vertex in V' in $G - V'$. An edge subset $E' \subseteq E(G)$ in a connected graph G is called *separating* (resp., *non-separating*) if $G - E'$ becomes disconnected (resp., $G - E'$ remains connected). The *rank* $r(G)$ of a graph G is defined to be the minimum $|F|$ of an edge subset $F \subseteq E(G)$ such that $G - F$ contains no cycle, where $r(G) = |E(G)| - |V(G)| + 1$ for a connected graph G . Observe that $r(G - E') = r(G) - |E'|$ holds for any non-separating edge subset $E' \subseteq E(G)$. An edge $e \in E(G)$ in a connected graph G is called a *bridge* if $\{e\}$ is separating. For a connected cyclic graph G , an edge e is called a *core-edge* if it is in a cycle of G or is a bridge $e = u_1u_2$ such that each of the connected graphs G_i , $i = 1, 2$ of $G - e$ contains a cycle. A vertex incident to a core-edge is called a *core-vertex* of G . A path with two end-vertices u and v is called a u, v -*path*.

We define a *rooted* graph to be a graph with a designated vertex, called a *root*. For a graph G possibly with a root, a *leaf-vertex* is defined to be a non-root vertex with degree 1. We call the edge uv incident to a leaf vertex v a *leaf-edge*, and denote by $V_{\text{leaf}}(G)$ and $E_{\text{leaf}}(G)$ the sets of leaf-vertices and leaf-edges in G , respectively. For a graph or a rooted graph G , we define graphs $G_i, i \in \mathbb{Z}_+$ obtained from G by removing the set of leaf-vertices i times so that

$$G_0 := G; \quad G_{i+1} := G_i - V_{\text{leaf}}(G_i),$$

where we call a vertex v a *tree vertex* if $v \in V_{\text{leaf}}(G_i)$ for some $i \geq 0$. Define the *height* $\text{ht}(v)$ of each tree vertex $v \in V_{\text{leaf}}(G_i)$ to be i ; and $\text{ht}(v)$ of each non-tree vertex v adjacent to a tree vertex to be $\text{ht}(u) + 1$ for the maximum $\text{ht}(u)$ of a tree vertex u adjacent to v , where we do not define height of any non-tree vertex not adjacent to any tree vertex. We call a vertex v with $\text{ht}(v) = k$ a *leaf k -branch*. The *height* $\text{ht}(T)$ of a rooted tree T is defined to be the maximum of $\text{ht}(v)$ of a vertex $v \in V(T)$. For an integer $k \geq 0$, we call a rooted tree T *k -lean* if T has at most one leaf k -branch. For an unrooted cyclic graph G , we regard that the set of non-core-edges in G induces a collection \mathcal{T} of trees each of which is rooted at a core-vertex, where we call G *k -lean* if each of the rooted trees in \mathcal{T} is k -lean.

2.1 Modeling of Chemical Compounds

We review a modeling of chemical compounds introduced by Zhu et al. [24].

To represent a chemical compound, we introduce a set of chemical elements such as H (hydrogen), C (carbon), O (oxygen), N (nitrogen) and so on. To distinguish a chemical element \mathbf{a} with multiple valences such as S (sulfur), we denote a chemical element \mathbf{a} with a valence i by $\mathbf{a}_{(i)}$, where we do not use such a suffix (i) for a chemical element \mathbf{a} with a unique valence. Let Λ be a set of chemical elements $\mathbf{a}_{(i)}$. For example, $\Lambda = \{\mathbf{H}, \mathbf{C}, \mathbf{O}, \mathbf{N}, \mathbf{P}, \mathbf{S}_{(2)}, \mathbf{S}_{(4)}, \mathbf{S}_{(6)}\}$. Let $\text{val} : \Lambda \rightarrow [1, 6]$ be a valence function. For example, $\text{val}(\mathbf{H}) = 1$, $\text{val}(\mathbf{C}) = 4$, $\text{val}(\mathbf{O}) = 2$, $\text{val}(\mathbf{P}) = 5$, $\text{val}(\mathbf{S}_{(2)}) = 2$, $\text{val}(\mathbf{S}_{(4)}) = 4$ and $\text{val}(\mathbf{S}_{(6)}) = 6$. For each chemical element $\mathbf{a} \in \Lambda$, let $\text{mass}(\mathbf{a})$ denote the mass of \mathbf{a} .

A chemical compound is represented by a *chemical graph* defined to be a tuple $\mathbb{C} = (H, \alpha, \beta)$ of a simple, connected undirected graph H and functions $\alpha : V(H) \rightarrow \Lambda$ and $\beta : E(H) \rightarrow [1, 3]$. The set of atoms and the set of bonds in the compound are represented by the vertex set $V(H)$ and the edge set $E(H)$, respectively. The chemical element assigned to a vertex $v \in V(H)$ is represented by $\alpha(v)$ and the bond-multiplicity between two adjacent vertices $u, v \in V(H)$ is represented by $\beta(e)$ of the edge $e = uv \in E(H)$. We say that two tuples $(H_i, \alpha_i, \beta_i), i = 1, 2$ are *isomorphic* if they admit an isomorphism ϕ , i.e., a bijection $\phi : V(H_1) \rightarrow V(H_2)$ such that $uv \in E(H_1), \alpha_1(u) = \mathbf{a}, \alpha_1(v) = \mathbf{b}, \beta_1(uv) = m \leftrightarrow \phi(u)\phi(v) \in E(H_2), \alpha_2(\phi(u)) = \mathbf{a}, \alpha_2(\phi(v)) = \mathbf{b}, \beta_2(\phi(u)\phi(v)) = m$. When H_i is rooted at a vertex $r_i, i = 1, 2$, these chemical graphs $(H_i, \alpha_i, \beta_i), i = 1, 2$ are *rooted-isomorphic* (r-isomorphic) if they admit an isomorphism ϕ such that $\phi(r_1) = r_2$.

For a notational convenience, we use a function $\beta_{\mathbb{C}} : V(H) \rightarrow [0, 12]$ for a chemical graph $\mathbb{C} = (H, \alpha, \beta)$ such that $\beta_{\mathbb{C}}(u)$ means the sum of bond-multiplicities of edges incident to a vertex u ; i.e.,

$$\beta_{\mathbb{C}}(u) \triangleq \sum_{uv \in E(H)} \beta(uv) \text{ for each vertex } u \in V(H).$$

For each vertex $u \in V(H)$, define the *electron-degree* $\text{eledeg}_{\mathbb{C}}(u)$ to be

$$\text{eledeg}_{\mathbb{C}}(u) \triangleq \beta_{\mathbb{C}}(u) - \text{val}(\alpha(u)).$$

For each vertex $u \in V(H)$, let $\text{deg}_{\mathbb{C}}(u)$ denote the number of vertices adjacent to u in \mathbb{C} .

For a chemical graph $\mathbb{C} = (H, \alpha, \beta)$, let $V_{\mathbf{a}}(\mathbb{C}), \mathbf{a} \in \Lambda$ denote the set of vertices $v \in V(H)$ such that $\alpha(v) = \mathbf{a}$ in \mathbb{C} and define the *hydrogen-suppressed chemical graph* $\langle \mathbb{C} \rangle$ to be the graph obtained from H by removing all the vertices $v \in V_{\mathbf{H}}(\mathbb{C})$.

2.2 Evaluating prediction function

We review the definition of coefficient of determination.

Let D be a data set of chemical graphs \mathbb{C} with an observed value $a(\mathbb{C}) \in \mathbb{R}$, where we denote by $a_i = a(\mathbb{C}_i)$ for an indexed graph \mathbb{C}_i .

Let f be a feature function that maps a chemical graph \mathbb{C} to a vector $f(\mathbb{C}) \in \mathbb{R}^K$ where we denote by $x_i = f(\mathbb{C}_i)$ for an indexed graph \mathbb{C}_i . For a prediction function $\eta : \mathbb{R}^K \rightarrow \mathbb{R}$, define an error function

$$\text{Err}(\eta; D) \triangleq \sum_{\mathbb{C}_i \in D} (a_i - \eta(f(\mathbb{C}_i)))^2 = \sum_{\mathbb{C}_i \in D} (a_i - \eta(x_i))^2,$$

and define the *coefficient of determination* $R^2(\eta, D)$ to be

$$R^2(\eta, D) \triangleq 1 - \frac{\text{Err}(\eta; D)}{\sum_{\mathbb{C}_i \in D} (a_i - \tilde{a})^2} \text{ for } \tilde{a} = \frac{1}{|D|} \sum_{\mathbb{C} \in D} a(\mathbb{C}).$$

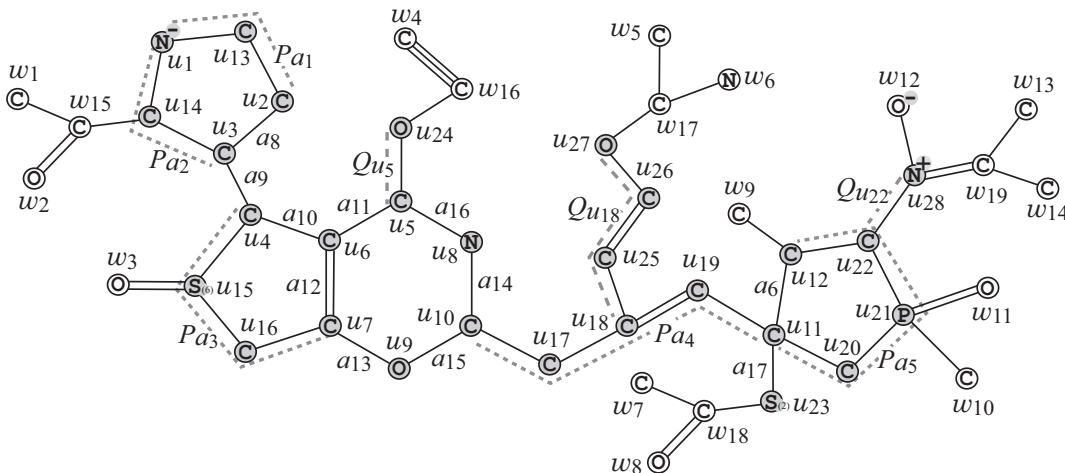


Figure 2: An illustration of a hydrogen-suppressed chemical graph $\langle \mathbb{C} \rangle$ obtained from a chemical graph \mathbb{C} with $r(\mathbb{C}) = 4$ by removing all the hydrogens, where for $\rho = 2$, $V^{\text{ex}}(\mathbb{C}) = \{w_i \mid i \in [1, 19]\}$ and $V^{\text{int}}(\mathbb{C}) = \{u_i \mid i \in [1, 28]\}$.

3 Two-layered Model

This section reviews the two-layered model introduced by Zhu et al. [24].

Let $\mathbb{C} = (H, \alpha, \beta)$ be a chemical graph and $\rho \geq 1$ be an integer, which we call a *branch-parameter*.

A *two-layered model* of \mathbb{C} is a partition of the hydrogen-suppressed chemical graph $\langle \mathbb{C} \rangle$ into an “interior” and an “exterior” in the following way. We call a vertex $v \in V(\langle \mathbb{C} \rangle)$ (resp., an edge $e \in E(\langle \mathbb{C} \rangle)$) of \mathbb{C} an *exterior-vertex* (resp., *exterior-edge*) if $\text{ht}(v) < \rho$ (resp., e is incident to an exterior-vertex) and denote the sets of exterior-vertices and exterior-edges by $V^{\text{ex}}(\mathbb{C})$ and $E^{\text{ex}}(\mathbb{C})$, respectively and denote $V^{\text{int}}(\mathbb{C}) = V(\langle \mathbb{C} \rangle) \setminus V^{\text{ex}}(\mathbb{C})$ and $E^{\text{int}}(\mathbb{C}) = E(\langle \mathbb{C} \rangle) \setminus E^{\text{ex}}(\mathbb{C})$, respectively. We call a vertex in $V^{\text{int}}(\mathbb{C})$ (resp., an edge in $E^{\text{int}}(\mathbb{C})$) an *interior-vertex* (resp., *interior-edge*). The set $E^{\text{ex}}(\mathbb{C})$ of exterior-edges forms a collection of connected graphs each of which is regarded as a rooted tree T rooted at the vertex $v \in V(T)$ with the maximum $\text{ht}(v)$. Let $\mathcal{T}^{\text{ex}}(\langle \mathbb{C} \rangle)$ denote the set of these chemical rooted trees in $\langle \mathbb{C} \rangle$. The *interior* \mathbb{C}^{int} of \mathbb{C} is defined to be the subgraph $(V^{\text{int}}(\mathbb{C}), E^{\text{int}}(\mathbb{C}))$ of $\langle \mathbb{C} \rangle$.

Figure 2 illustrates an example of a hydrogen-suppressed chemical graph $\langle \mathbb{C} \rangle$. For a branch-parameter $\rho = 2$, the interior of the chemical graph $\langle \mathbb{C} \rangle$ in Figure 2 is obtained by removing the set of vertices with degree 1 $\rho = 2$ times; i.e., first remove the set $V_1 = \{w_1, w_2, \dots, w_{14}\}$ of vertices of degree 1 in $\langle \mathbb{C} \rangle$ and then remove the set $V_2 = \{w_{15}, w_{16}, \dots, w_{19}\}$ of vertices of degree 1 in $\langle \mathbb{C} \rangle - V_1$, where the removed vertices become the exterior-vertices of $\langle \mathbb{C} \rangle$.

For each interior-vertex $u \in V^{\text{int}}(\mathbb{C})$, let $T_u \in \mathcal{T}^{\text{ex}}(\langle \mathbb{C} \rangle)$ denote the chemical tree rooted at u (where possibly T_u consists of vertex u) and define the ρ -fringe-tree $\mathbb{C}[u]$ to be the chemical rooted tree obtained from T_u by putting back the hydrogens originally attached with T_u in \mathbb{C} . Let $\mathcal{T}(\mathbb{C})$ denote the set of ρ -fringe-trees $\mathbb{C}[u], u \in V^{\text{int}}(\mathbb{C})$. Figure 3 illustrates the set $\mathcal{T}(\mathbb{C}) = \{\mathbb{C}[u_i] \mid i \in [1, 28]\}$ of the 2-fringe-trees of the example \mathbb{C} with $\langle \mathbb{C} \rangle$ in Figure 2.

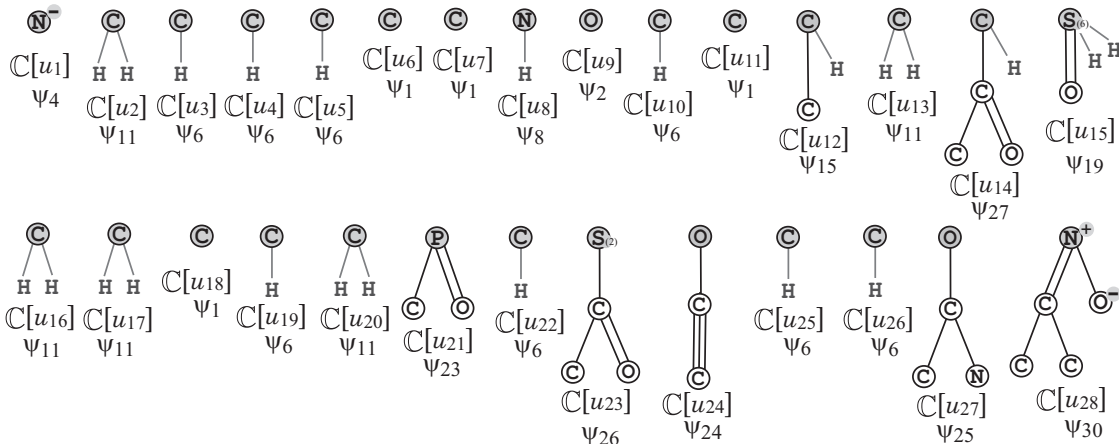


Figure 3: The set $\mathcal{T}(\mathbb{C})$ of 2-fringe-trees $\mathbb{C}[u_i], i \in [1, 28]$ of the example \mathbb{C} with $\langle \mathbb{C} \rangle$ in Figure 2, where the root of each tree is depicted with a gray circle and the hydrogens attached to non-root vertices are omitted in the figure.

Feature Function The feature of an interior-edge $e = uv \in E^{\text{int}}(\mathbb{C})$ such that $\alpha(u) = \mathbf{a}$, $\deg_{\langle \mathbb{C} \rangle}(u) = d$, $\alpha(v) = \mathbf{b}$, $\deg_{\langle \mathbb{C} \rangle}(v) = d'$ and $\beta(e) = m$ is represented by a tuple $(ad, \mathbf{b}d', m)$, which is called the *edge-configuration* of the edge e , where we call the tuple $(\mathbf{a}, \mathbf{b}, m)$ the *adjacency-configuration* of the edge e .

For an integer K , a feature vector $f(\mathbb{C})$ of a chemical graph \mathbb{C} is defined by a *feature function* f that consists of K descriptors. We call \mathbb{R}^K the *feature space*.

Tanaka et al. [23] defined a feature vector $f(\mathbb{C}) \in \mathbb{R}^K$ to be a combination of the frequency of edge-configurations of the interior-edges and the frequency of chemical rooted trees among the set of chemical rooted trees $\mathbb{C}[u]$ over all interior-vertices u .

Topological Specification A topological specification is described as a set of the following rules proposed by Shi et al. [22] and modified by Tanaka et al. [23]:

- (i) a *seed graph* $G_{\mathbb{C}}$ as an abstract form of a target chemical graph \mathbb{C} ;
- (ii) a set \mathcal{F} of chemical rooted trees as candidates for a tree $\mathbb{C}[u]$ rooted at each interior-vertex u in \mathbb{C} ; and
- (iii) lower and upper bounds on the number of components in a target chemical graph such as chemical elements, double/triple bonds and the interior-vertices in \mathbb{C} .

Figure 4(a) and (b) illustrate examples of a seed graph $G_{\mathbb{C}}$ and a set \mathcal{F} of chemical rooted trees, respectively. Given a seed graph $G_{\mathbb{C}}$, the interior of a target chemical graph \mathbb{C} is constructed from $G_{\mathbb{C}}$ by replacing some edges $a = uv$ with paths P_a between the end-vertices u and v and by attaching new paths Q_v to some vertices v . For example, a chemical graph \mathbb{C} with $\langle \mathbb{C} \rangle$ in Figure 2 is constructed from the seed graph $G_{\mathbb{C}}$ in Figure 4(a) as follows.

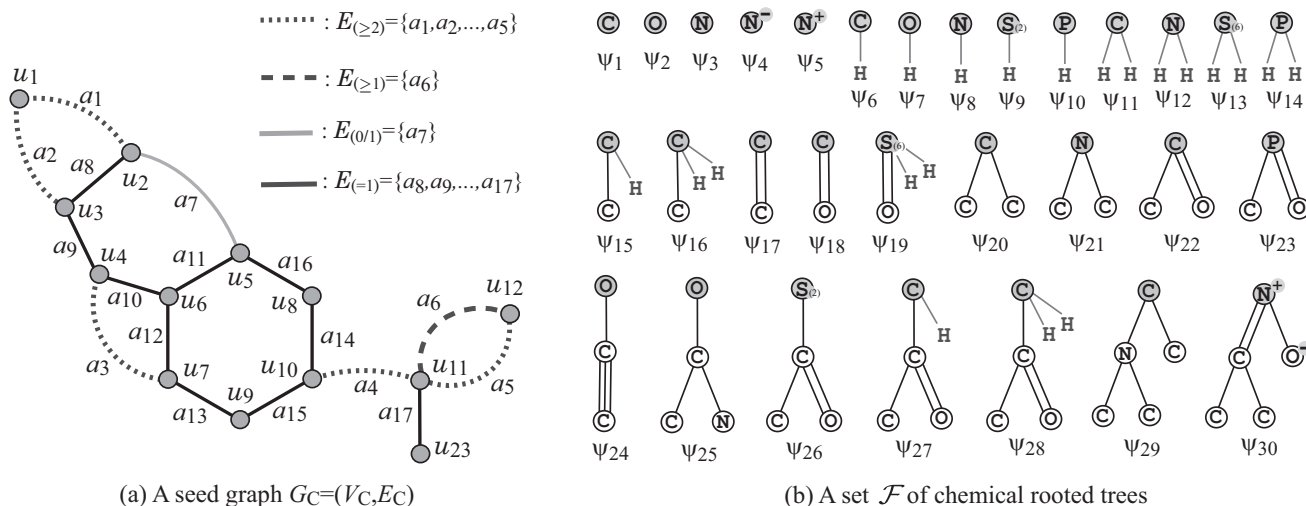


Figure 4: (a) An illustration of a seed graph G_C with $r(G_C) = 5$, where the vertices in V_C are depicted with gray circles, the edges in $E_{(\geq 2)}$ are depicted with dotted lines, the edges in $E_{(\geq 1)}$ are depicted with dashed lines, the edges in $E_{(0/1)}$ are depicted with gray bold lines and the edges in $E_{(=)}$ are depicted with black solid lines; (b) A set $\mathcal{F} = \{\psi_1, \psi_2, \dots, \psi_{30}\} \subseteq \mathcal{F}(D_\pi)$ of 30 chemical rooted trees $\psi_i, i \in [1, 30]$, where the root of each tree is depicted with a gray circle, where the hydrogens attached to non-root vertices are omitted in the figure.

- First replace five edges $a_1 = u_1u_2, a_2 = u_1u_3, a_3 = u_4u_7, a_4 = u_{10}u_{11}$ and $a_5 = u_{11}u_{12}$ in G_C with new paths $P_{a_1} = (u_1, u_{13}, u_2), P_{a_2} = (u_1, u_{14}, u_3), P_{a_3} = (u_4, u_{15}, u_{16}, u_7), P_{a_4} = (u_{10}, u_{17}, u_{18}, u_{19}, u_{11})$ and $P_{a_5} = (u_{11}, u_{20}, u_{21}, u_{22}, u_{12})$, respectively to obtain a subgraph G_1 of $\langle \mathbb{C} \rangle$.
- Next attach to this graph G_1 three new paths $Q_{u_5} = (u_5, u_{24}), Q_{u_{18}} = (u_{18}, u_{25}, u_{26}, u_{27})$ and $Q_{u_{22}} = (u_{22}, u_{28})$ to obtain the interior of $\langle \mathbb{C} \rangle$ in Figure 2.
- Finally attach to the interior 28 trees selected from the set \mathcal{F} and assign chemical elements and bond-multiplicities in the interior to obtain a chemical graph \mathbb{C} with $\langle \mathbb{C} \rangle$ in Figure 2. In Figure 3, $\psi_1 \in \mathcal{F}$ is selected for $\mathbb{C}[u_i], i \in \{6, 7, 11\}$. Similarly ψ_2 for $\mathbb{C}[u_9], \psi_4$ for $\mathbb{C}[u_1], \psi_6$ for $\mathbb{C}[u_i], i \in \{3, 4, 5, 10, 19, 22, 25, 26\}, \psi_8$ for $\mathbb{C}[u_8], \psi_{11}$ for $\mathbb{C}[u_i], i \in \{2, 13, 16, 17, 20\}, \psi_{15}$ for $\mathbb{C}[u_{12}], \psi_{19}$ for $\mathbb{C}[u_{15}], \psi_{23}$ for $\mathbb{C}[u_{21}], \psi_{24}$ for $\mathbb{C}[u_{24}], \psi_{25}$ for $\mathbb{C}[u_{27}], \psi_{26}$ for $\mathbb{C}[u_{23}], \psi_{27}$ for $\mathbb{C}[u_{14}]$ and ψ_{30} for $\mathbb{C}[u_{28}]$.

Our definition of a topological specification is analogous with the one by Tanaka et al. [23] except for a necessary modification due to the introduction of multiple valences of chemical elements, cations and anions (see Appendix B for a full description of topological specification).

4 Grid Neighbor Search

This section introduces a procedure of generating solutions of an MILP as a new building block of the framework of inferring chemical graphs.

For a notational convenience, let $(x, 1)$ for a vector $x \in \mathbb{R}^K$ denote the vector $y \in \mathbb{R}^{K+1}$ such

that $y(j) = x(j), j \in [1, K]$ and $y(K + 1) = 1$.

Choose an integer $p_{\max} \geq 1$ as the dimension of a search space $\mathbb{R}^{p_{\max}}$, a vector $s^* \in \mathbb{R}^{p_{\max}}$ as the center of $\mathbb{R}^{p_{\max}}$ and a vector $\delta \in \mathbb{R}_+^{p_{\max}}$ with $\delta(p) > 0, p \in [1, p_{\max}]$ as the width of a grid in the space $\mathbb{R}^{p_{\max}}$. A *grid* is defined to be an integer vector $z \in \mathbb{Z}^{p_{\max}}$ for which we define a subspace $S(z) \subseteq \mathbb{R}^{p_{\max}}$ to be

$$S(z) \triangleq \{s \in \mathbb{R}^{p_{\max}} \mid s^*(p) + (z(p) - 0.5)\delta(p) \leq s(p) \leq s^*(p) + (z(p) + 0.5)\delta(p), p \in [1, p_{\max}]\}.$$

We call a grid $z \in \mathbb{Z}^{p_{\max}}$ with $z(p) = 0, p \in [1, p_{\max}]$ the *center grid*. A neighbor $N(r)$ of the center with a radius vector $r \in \mathbb{Z}_+^{p_{\max}}$ is defined to be a set of grids such that

$$N(r) \triangleq \{z \in \mathbb{Z}^{p_{\max}} \mid -r(p) \leq z(p) \leq r(p), p \in [1, p_{\max}]\}.$$

Let us introduce a partial order \preceq over the set $\mathbb{Z}^{p_{\max}}$ of grids. For two grids $z, z' \in \mathbb{Z}^{p_{\max}}$, $z' \preceq z$ if $0 \leq z'(p) \leq z(p)$ or $0 \geq z'(p) \geq z(p)$ for each $p \in [1, p_{\max}]$, where we let $z' \prec z$ mean that $z' \preceq z$ and $z' \neq z$.

We introduce a linear function $\theta_p : \mathbb{R}^K \rightarrow \mathbb{R}$ for each $p \in [1, p_{\max}]$, called a *projection function* such that

$$\theta_p(x) \triangleq w_p \cdot (x, 1) = \sum_{j \in [1, K]} w_p(j)x(j) + w_p(K + 1)$$

by choosing a vector $w_p \in \mathbb{R}^{K+1}$. For a notational convenience, let $\theta(x), x \in \mathbb{R}^K$ denote the vector $(\theta_1(x), \theta_2(x), \dots, \theta_{p_{\max}}(x)) \in \mathbb{R}^{p_{\max}}$.

In the framework of inferring chemical graphs, we formulate an MILP $\mathcal{M}(g, x, y; \mathcal{C}_1, \mathcal{C}_2)$ that consists of two MILPs $\mathcal{M}(x, y; \mathcal{C}_1)$ and $\mathcal{M}(g, x; \mathcal{C}_2)$, where the former simulates the computation process of a prediction function η for a chemical property π and the latter simulates the computation process of a feature function f and describes construction of a chemical graph that satisfies a given topological specification σ . By solving the MILP for lower and upper bounds on a target value of π , we obtain a desired chemical graph \mathbb{C}^\dagger when the MILP instance is feasible (or we detect that there is no such chemical graph when the instance is infeasible).

We design a procedure for finding other solutions of the MILP by searching the neighbor of the output chemical graph \mathbb{C}^\dagger . Suppose that we have chosen a dimension p_{\max} , a width vector $\delta \in \mathbb{R}_+^{p_{\max}}$ with $\delta(p) > 0, p \in [1, p_{\max}]$, a radius vector $r \in \mathbb{Z}_+^{p_{\max}}$ and projection functions $\theta_p, p \in [1, p_{\max}]$.

1. Let \underline{y}^* and \overline{y}^* be lower and upper bounds on the value of property π of a chemical graph to be inferred. We first solve $\mathcal{M}(g, x, y; \mathcal{C}_1, \mathcal{C}_2)$ with the input values $(\underline{y}^*, \overline{y}^*)$ to find a desired chemical graph \mathbb{C}^\dagger . (When the MILP instance is infeasible, we halt.) Let $x^* := f(\mathbb{C}^\dagger) \in \mathbb{R}^K$.
2. Set the center of the space $\mathbb{R}^{p_{\max}}$ to be $s^* := \theta(x^*)$. For each grid $z \in N(r)$, we solve an MILP $\mathcal{M}(g, x, y; \mathcal{C}_1, \mathcal{C}_2)$ with an additional linear constraint $\theta(x) \in S(z)$ for $(\underline{y}^*, \overline{y}^*)$, where we call a grid z *feasible* (resp., *infeasible*) if the augmented MILP instance is feasible (resp., infeasible).
3. For each feasible grid $z \in N(r)$, output a feasible solution \mathbb{C}_z^\dagger of the augmented MILP instance. We check the feasibility of grids $z \in N(r)$ in a non-decreasing order of $\max_{p \in [1, p_{\max}]} |z(p)|$,

and discard any grid $z \in N(r)$ without testing the feasibility of z if we find an infeasible grid $z' \in N(r)$ with $z' \prec z$. Note that \mathbb{C}_z^\dagger and $\mathbb{C}_{z'}^\dagger$ are not isomorphic unless $\theta(f(\mathbb{C}_z^\dagger))$ and $\theta(f(\mathbb{C}_{z'}^\dagger))$ happen to belong to the common boundary $S(z) \cap S(z')$.

In the above method, we can choose arbitrarily many grids in the space of $\mathbb{R}^{p_{\max}}$ around the center s^* by choosing small $\delta(p)$ and large $r(p)$, $p \in [1, p_{\max}]$, where each $\delta(p)$ needs to be large enough to avoid a possible numerical error.

We can also choose arbitrary linear functions as projection functions θ_p , $p \in [1, p_{\max}]$. When we have constructed a prediction function η_τ as a linear function with linear regression for several chemical properties τ other than the current target property π , we can use such functions as projection functions. For example, if a linear prediction function η_τ is available for a chemical property τ such as solubility (SL) and lipophilicity (LP), then we can infer chemical graphs \mathbb{C}_z^\dagger with slightly different values of these properties $\tau_1 = \text{SL}$ and $\tau_2 = \text{LP}$ by setting $\theta_p := \eta_{\tau_p}$, $p = 1, 2$.

5 Results

We implemented our method of Stages 1 to 5 for inferring chemical graphs under a given topological specification and conducted experiments to evaluate the computational efficiency. We executed the experiments on a PC with Processor: Core i7-9700 (3.0GHz; 4.7 GHz at the maximum) and Memory: 16 GB RAM DDR4. To construct an ANN, we used `scikit-learn` version 0.23.2 with Python 3.8.5, MLPRegressor and ReLU activation function.

Results on Phase 1. We implemented Stages 1, 2 and 3 in Phase 1 as follows.

We have conducted experiments of Lasso linear regression and for 37 chemical properties of monomers (resp., ten chemical properties of polymers) using the same feature function in this paper and we found that the test coefficient of determination R^2 exceeds 0.927 for the following 11 properties of monomers: octanol/water partition coefficient (KOW), heat of combustion (HC), vapor density (VD), electron density on the most positive atom (EDPA), heat of atomization (HA), heat of formation (HF), internal energy at 0K (U0), isotropic polarizability (ALPHA), heat capacity at 298.15K (Cv), isobaric heat capacities in liquid phase (IHCLIQ) and isobaric heat capacities in solid phase (IHCSOL) (see [24] for the details) and that the test coefficient of determination R^2 exceeds 0.9 for the following five properties of polymers: experimental amorphous density (AMD), heat capacity liquid (HCL), heat capacity solid (HCS), mol volume (MLV) and glass transition (TG) (see [25] for the details). We excluded the above properties in our experiment of constructing prediction functions with ANNs.

We have conducted experiments of ANNs for the rest of 26 chemical properties of monomers (resp., five chemical properties of polymers) among which we report the following 12 properties of monomers (resp., two properties of polymers) to which the test coefficient of determination R^2 by ANNs is better than that by Lasso linear regression: biological half life (BHL), boiling point (BP), critical pressure (CP), dissociation constants (DC), flash point (FP), Kovats retention index (KOV), lipophilicity (LP), energy of lowest unoccupied molecular orbital (LUMO), optical rotation (OPTR), solubility (SL), surface tension (SFT) and viscosity (VIS) (resp., characteristic ratio (CHAR) and refractive index (RFID)). We explain the data set and the results for these 14 properties in detail below.

We used data sets of monomers provided by HSDB from PubChem [26] for BHL, CP, DC, FP and OPTR, M. Jalali-Heravi and M. Fatemi [27] for KOV, Roy and Saha [28] for BP, MoleculeNet [34] for LUMO, Goussard et al. [30] for SFT, Goussard et al. [31] for VIS and Figshare [33] for LP. Property LUMO has the original data set D^* with more than 130,000 compounds, and we used a set D_π of 1,000 graphs randomly selected from D^* as a data set of property LUMO in this experiment.

We used data sets of polymers provided by Bicerano [35], where we did not include any polymer whose chemical formula could not be found by its name in the book. For property CHAR (resp., RFID), we remove the following polymer as an outlier from the original data set: ethyleneTerephthalate, oxy(2-methyl-6-phenyl-1,4-phenylene) and N-vinylCarbazole (resp., 2-decyl-1,4-butadiene).

Stage 1. We set a graph class \mathcal{G} to be the set of all chemical graphs with any graph structure, and set a branch-parameter ρ to be 2.

For each of the properties, we first select a set Λ of chemical elements and then collect a data set D_π on chemical graphs over the set Λ of chemical elements. To construct the data set D_π , we eliminated chemical compounds that do not satisfy one of the following: the graph is connected, the number of carbon atoms is at least four, and the number of non-hydrogen neighbors of each atom is at most 4.

Stage 2. We used the new feature function defined in our chemical model without suppressing hydrogen (see Appendix A for the detail). We normalize the range of each descriptor and the range $\{t \in \mathbb{R} \mid \underline{a} \leq t \leq \bar{a}\}$ of property values $a(\mathbb{C}), \mathbb{C} \in D_\pi$.

Table 1 shows the size and range of data sets that we prepared for each chemical property in Stages 1 and 2, where we denote the following:

- Λ : the set of elements used in the data set D_π ; Λ is one of the following nine sets: $\Lambda_1 = \{\text{H, C, O}\}$; $\Lambda_2 = \{\text{H, C, O, N}\}$; $\Lambda_3 = \{\text{H, C, O, Si}_{(4)}\}$; $\Lambda_4 = \{\text{H, C, O, N, S}_{(2)}, \text{F}\}$; $\Lambda_5 = \{\text{H, C, O, N, Cl, Pb}\}$; $\Lambda_6 = \{\text{H, C, O, N, S}_{(2)}, \text{S}_{(6)}, \text{Cl}\}$; $\Lambda_7 = \{\text{H, C, O, N, S}_{(2)}, \text{S}_{(4)}, \text{S}_{(6)}, \text{Cl}\}$; $\Lambda_8 = \{\text{H, C}_{(2)}, \text{C}_{(3)}, \text{C}_{(4)}, \text{C}_{(5)}, \text{O}, \text{N}_{(1)}, \text{N}_{(2)}, \text{N}_{(3)}, \text{F}\}$; $\Lambda_9 = \{\text{H, C, O}_{(1)}, \text{O}_{(2)}, \text{N}\}$; $\Lambda_{10} = \{\text{H, C, O, N, Si}_{(4)}, \text{Cl, Br}\}$; $\Lambda_{11} = \{\text{H, C, O}_{(1)}, \text{O}_{(2)}, \text{N, Si}_{(4)}, \text{Cl, F}\}$; and $\Lambda_{12} = \{\text{H, C, O}_{(1)}, \text{O}_{(2)}, \text{N, Si}_{(4)}, \text{Cl, F, S}_{(2)}, \text{S}_{(6)}, \text{Br}\}$, where $\mathbf{a}_{(i)}$ for a chemical element \mathbf{a} and an integer $i \geq 1$ means that a chemical element \mathbf{a} with valence i .
- $|D_\pi|$: the size of data set D_π over Λ for the property π .
- \underline{n}, \bar{n} : the minimum and maximum values of the number $n(\mathbb{C})$ of non-hydrogen atoms in the compounds \mathbb{C} in D_π .
- \underline{a}, \bar{a} : the minimum and maximum values of $a(\mathbb{C})$ for π over the compounds \mathbb{C} in D_π .
- $|\Gamma|$: the number of different edge-configurations of interior-edges over the compounds in D_π .
- $|\mathcal{F}|$: the number of non-isomorphic chemical rooted trees in the set of all 2-fringe-trees in the compounds in D_π .
- K : the number of descriptors in the original feature vector $f(\mathbb{C})$.

Stage 3. For each chemical property π , we conducted a preliminary experiment to choose the following: a subset S_π of the original set of K descriptors; an architecture A_π with at most five hidden layers; a nonnegative real $\rho_\pi^{\text{stp}} \leq 1$; and an integer $\text{ite}_\pi^{\text{stp}}$, where we will use ρ_π^{stp} and $\text{ite}_\pi^{\text{stp}}$ as parameters to execute an early stopping in constructing a prediction function with a training data set. Let f_π denote the feature vector that consists of the descriptors in the set S_π .

For each property π , we conducted ten 5-fold cross-validations. In a 5-fold cross-validation, we construct five prediction functions $\eta^{(k)}, k \in [1, 5]$ as follows. Partition data set D_π into five subsets $D_\pi^{(k)}, k \in [1, 5]$ randomly. For each $k \in [1, 5]$, use the set $D_{\text{train}} := D_\pi \setminus D_\pi^{(k)}$ as a training set and construct an ANN on the selected architecture A_π with the feature vector f_π by the MLPRegressor of `scikit-learn`, where we stop updating weights/biases on A_π during an execution of the iterative algorithm when the coefficient of determination $R^2(\eta, D_{\text{train}})$ of the prediction function η by the current weights/biases exceeds ρ_π^{stp} (where we terminate the execution when the number of iterations exceeds $1.5 \times \text{ite}_\pi^{\text{stp}}$ even if $R^2(\eta, D_{\text{train}})$ does not reach ρ_π^{stp}). Set $\eta^{(k)}$ to be the prediction function η by the resulting weights/biases on A_π . We evaluate the performance of the prediction function $\eta^{(k)}$ with the coefficient $R^2(\eta^{(k)}, D_{\text{test}})$ of determination for the test set $D_{\text{test}} := D_\pi^{(k)}$. The running time per trial in a cross-validation was at most 8.4 seconds.

Table 1: Results of Stages 1 and 2 in Phase 1.

π	Λ	$ D_\pi $	\underline{n}, \bar{n}	\underline{a}, \bar{a}	$ \Gamma $	$ \mathcal{F} $	K
BHL	Λ_2	300	5, 36	0.03, 732.99	20	70	120
BHL	Λ_7	514	5, 36	0.03, 732.99	26	101	166
BP	Λ_2	370	4, 67	-11.7, 470.0	22	130	184
BP	Λ_6	444	4, 67	-11.7, 470.0	26	163	230
CP	Λ_2	125	4, 63	$4.7 \times 10^{-6}, 5.52$	8	75	112
CP	Λ_5	131	4, 63	$4.7 \times 10^{-6}, 5.52$	8	79	119
DC	Λ_2	141	5, 44	0.5, 17.11	20	62	111
DC	Λ_6	161	5, 44	0.5, 17.11	25	69	130
FP	Λ_2	368	4, 67	-82.99, 300.0	20	131	183
FP	Λ_6	424	4, 67	-82.99, 300.0	25	161	229
KOV	Λ_1	52	11, 16	1422.0, 1919.0	9	33	64
LP	Λ_2	615	6, 60	-3.62, 6.84	32	116	186
LP	Λ_7	936	6, 74	-3.62, 6.84	44	136	231
LUMO	Λ_8	977	6, 9	-0.1144, 0.1026	59	190	297
OPTR	Λ_2	147	5, 44	-117.0, 165.0	21	55	107
OPTR	Λ_4	157	5, 69	-117.0, 165.0	25	62	123
SL	Λ_2	673	4, 55	-9.332, 1.11	27	154	217
SL	Λ_7	915	4, 55	-11.6, 1.11	42	207	300
SFT	Λ_3	247	5, 33	12.3, 45.1	11	91	128
VIS	Λ_3	282	5, 36	-0.64, 1.63	12	88	126
CHAR	Λ_2	27	4, 18	5.5, 13.2	22	17	67
CHAR	Λ_{10}	32	4, 18	5.5, 13.2	26	21	82
RFID	Λ_9	91	4, 29	1.339, 1.683	26	35	96
RFID	Λ_{11}	124	4, 29	1.339, 1.683	32	50	124
RFID	Λ_{12}	134	4, 29	1.339, 1.71	38	56	144

Table 2 shows the results on Stage 3, where we denote the following:

Table 2: Results of Stage 3 in Phase 1.

π	$ D_\pi $	A_π	ρ_π^{stp}	ANN R^2	LLR R^2
BHL	300	(108, 64, 64, 64, 64, 64, 1)	0.86	0.630	0.364
BHL	514	(46, 10, 8, 1)	0.71	0.622	0.483
BP	370	(71, 28, 22, 17, 13, 10, 1)	0.93	0.765	0.599
BP	444	(225, 135, 135, 135, 135, 135, 1)	0.98	0.720	0.663
CP	125	(19, 10, 10, 10, 1)	0.66	0.694	0.445
CP	131	(19, 10, 10, 10, 1)	0.66	0.727	0.556
DC	141	(53, 10, 8, 1)	0.93	0.651	0.489
DC	161	(109, 87, 87, 87, 87, 1)	0.94	0.622	0.574
FP	368	(30, 10, 10, 10, 10, 10, 1)	0.88	0.746	0.589
FP	424	(42, 16, 16, 16, 16, 1)	0.90	0.733	0.571
KOV	52	(28, 10, 10, 1)	0.92	0.727	0.677
LP	615	(186, 74, 74, 74, 74, 74, 1)	0.98	0.867	0.856
LP	936	(197, 157, 157, 157, 157, 157, 1)	0.81	0.859	0.840
LUMO	977	(241, 192, 192, 192, 192, 192, 1)	0.99	0.860	0.841
OPTR	147	(107, 64, 51, 40, 32, 1)	0.97	0.919	0.823
OPTR	157	(114, 20, 10, 1)	0.96	0.894	0.825
SL	673	(205, 10, 5, 1)	0.94	0.819	0.772
SL	915	(126, 25, 25, 25, 1)	0.95	0.822	0.808
SFT	247	(19, 15, 12, 9, 1)	0.91	0.834	0.804
VIS	282	(19, 11, 8, 6, 5, 1)	0.97	0.929	0.893
CHAR	27	(38, 22, 22, 22, 22, 22, 1)	0.98	0.641	0.431
CHAR	32	(38, 15, 15, 15, 1)	0.90	0.622	0.235
RfID	91	(31, 18, 14, 11, 8, 6, 1)	0.95	0.871	0.852
RfID	124	(60, 48, 38, 30, 24, 1)	0.90	0.891	0.832
RfID	134	(53, 42, 33, 26, 1)	0.94	0.866	0.832

- A_π : an architecture A_π used to construct a prediction function for property π , where $(K', p_1, p_2, \dots, p_\ell, 1)$ means an architecture with an input layer with K' nodes, ℓ hidden layers with $p_i, i \in [1, \ell]$ nodes and an output layer with a single node, where K' is the size $|S_\pi|$ of the set S_π of selected descriptors from the original set of K descriptors.
- ρ_π^{stp} : a nonnegative real with $0 \leq \rho_\pi^{\text{stp}} \leq 1$ by which we execute an early stopping in constructing a prediction function with a training data set.
- ANN R^2 : the median of test R^2 over all 50 trials in ten 5-fold cross-validations for prediction functions constructed with ANNs in this paper.
- LLR R^2 : the median of test R^2 over all 50 trials in ten 5-fold cross-validations for prediction functions constructed with Lasso linear regression [24].

Results on Phase 2. To execute Stages 4 and 5 in Phase 2, we used a set of seven instances $I_a, I_b^i, i \in [1, 4], I_c$ and I_d based on the seed graphs prepared by Zhu et al. [24]. We here present their

seed graphs G_C (see Appendix B for the details of I_a and Appendix C for the details of $I_b^i, i \in [1, 4]$, I_c and I_d).

The seed graph G_C of I_a is given by the graph in Figure 4(a). The seed graph G_C^1 of I_b^1 (resp., $G_C^i, i = 2, 3, 4$ of $I_b^i, i = 2, 3, 4$) is illustrated in Figure 5.

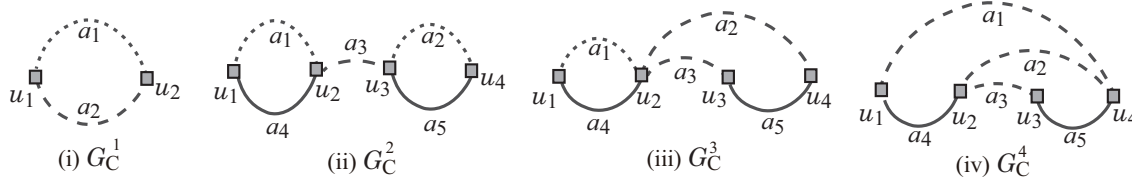


Figure 5: (i) Seed graph G_C^1 for I_b^1 and I_d ; (ii) Seed graph G_C^2 for I_b^2 ; (iii) Seed graph G_C^3 for I_b^3 ; (iv) Seed graph G_C^4 for I_b^4 .

Instance I_c has been introduced in order to infer a chemical graph \mathbb{C}^\dagger such that the core of \mathbb{C}^\dagger is equal to the core of chemical graph \mathbb{C}_A : CID 24822711 in Figure 6(a) and the frequency of each edge-configuration in the non-core of \mathbb{C}^\dagger is equal to that of chemical graph \mathbb{C}_B : CID 59170444 in Figure 6(b). This means that the seed graph G_C of I_c is the core of \mathbb{C}_A which is indicated by a shaded area in Figure 6(a).

Instance I_d has been introduced in order to infer a chemical monocyclic graph \mathbb{C}^\dagger such that the frequency vector of edge-configurations in \mathbb{C}^\dagger is a vector obtained by merging those of chemical graphs \mathbb{C}_A : CID 10076784 and \mathbb{C}_B : CID 44340250 in Figure 6(c) and (d), respectively. The seed graph G_C of I_d is given by G_C^1 in Figure 5(i).

Stage 4. We executed Stage 4 for three properties $\pi \in \{\text{FP}, \text{OPTR}, \text{SFT}\}$.

For the MILP formulation $\mathcal{M}(x, y; \mathcal{C}_1)$, we use the prediction function that attained the median test R^2 in Table 2. To solve an MILP in Stage 4, we used CPLEX version 12.10. Tables 3 and 5 show the computational results of the experiment in Stage 4 for the five properties, where we denote the following:

- n_{LB} : a lower bound on the number of non-hydrogen atoms in a chemical graph \mathbb{C} to be inferred;
- $\underline{y}^*, \overline{y}^*$: lower and upper bounds $\underline{y}^*, \overline{y}^* \in \mathbb{R}$ on the value $a(\mathbb{C})$ of a chemical graph \mathbb{C} to be inferred;
- $\#v$ (resp., $\#c$): the number of variables (resp., constraints) in the MILP in Stage 4;
- I-time: the time (sec.) to solve the MILP in Stage 4;
- n : the number $n(\mathbb{C}^\dagger)$ of non-hydrogen atoms in the chemical graph \mathbb{C}^\dagger inferred in Stage 4;
- n^{int} : the number $n^{\text{int}}(\mathbb{C}^\dagger)$ of interior-vertices in the chemical graph \mathbb{C}^\dagger inferred in Stage 4; and
- η : the predicted property value $\eta(f(\mathbb{C}^\dagger))$ of the chemical graph \mathbb{C}^\dagger inferred in Stage 4.

Figure 7(a) illustrates the chemical graph \mathbb{C}^\dagger inferred from I_a with $(\underline{y}^*, \overline{y}^*) = (130, 133)$ of FP in Table 3.

Figure 7(b) illustrates the chemical graph \mathbb{C}^\dagger inferred from I_b^2 with $(\underline{y}^*, \overline{y}^*) = (50, 52)$ of OPTR in Table 4.

Figure 7(c) illustrates the chemical graph \mathbb{C}^\dagger inferred from I_c with $(\underline{y}^*, \overline{y}^*) = (44, 45)$ of SFT in Table 5.

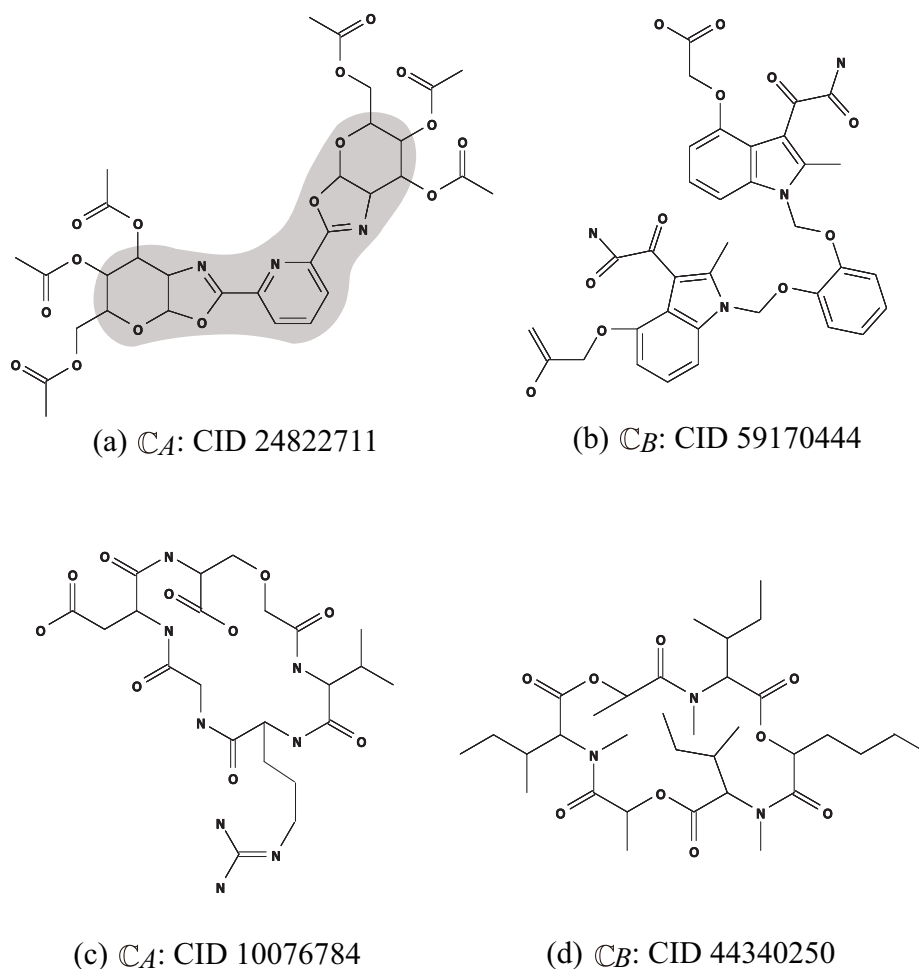


Figure 6: An illustration of chemical compounds for instances I_c and I_d : (a) \mathbb{C}_A : CID 24822711; (b) \mathbb{C}_B : CID 59170444; (c) \mathbb{C}_A : CID 10076784; (d) \mathbb{C}_B : CID 44340250, where hydrogens are omitted.

Table 3: Results of Stages 4 and 5 for FP.

inst.	n_{LB}	y^*, \bar{y}^*	$\#v$	$\#c$	I-time	n	n^{int}	η	D-time	C-LB	$\#\mathbb{C}$
I_a	30	130, 133	10877	10604	13.7	42	25	132.827	0.0703	1	1
I_b^1	10	110, 113	10773	8255	1.99	10	7	112.428	0.0234	2	2
I_b^2	20	215, 218	13217	11366	44.1	49	25	217.597	0.594	1.9E4	100
I_b^3	30	110, 113	12993	11346	43.6	48	30	110.193	17.2	2.4E7	100
I_b^4	40	137, 140	12767	11324	148.0	44	25	138.116	0.16	948	100
I_c	40	150, 153	7900	8629	4.38	50	34	151.133	0.0197	1	1
I_d	40	-63, -61	6507	8106	33.2	45	23	-61.733	251.0	4.9E9	100

In this experiment, we prepared several different types of instances: instances I_a and I_c have restricted seed graphs, the other instances have abstract seed graphs and instances I_c and I_d have

Table 4: Results of Stages 4 and 5 for OPTR.

inst.	n_{LB}	$\underline{y}^*, \overline{y}^*$	#v	#c	I-time	n	n^{int}	η	D-time	C-LB	#C
I_a	30	81, 83	10036	10396	4.32	47	26	81.587	0.066	2	2
I_b^1	10	-78, -76	10570	8128	103.52	19	15	-78.0	0.176	60	60
I_b^2	20	50, 52	12952	11231	41.2	49	25	51.452	0.21	1616	100
I_b^3	30	30, 32	12722	11201	37.3	50	25	31.261	0.186	210	100
I_b^4	40	116, 118	12491	11171	17.7	49	25	117.918	0.883	3.7E4	100
I_c	40	-30, -28	7885	8493	4.84	49	33	-29.163	0.0159	1	1
I_d	40	40, 42	6495	7976	10.5	40	23	40.152	2.52	7.3E5	100

Table 5: Results of Stages 4 and 5 for SFT.

inst.	n_{LB}	$\underline{y}^*, \overline{y}^*$	#v	#c	I-time	n	n^{int}	η	D-time	C-LB	#C
I_a	30	40, 41	9288	10207	2.10	41	22	40.231	0.0638	1	1
I_b^1	10	28, 29	7965	7599	2.28	11	5	28.488	0.00927	1	1
I_b^2	20	42, 43	9583	10719	12.0	48	25	42.998	0.163	200	100
I_b^3	30	36, 37	9326	10700	9.87	42	25	36.358	9.39	9.2E4	100
I_b^4	40	43, 44	9069	10682	13.4	46	25	43.857	0.123	116	100
I_c	40	44, 45	7777	8378	4.37	45	32	44.557	0.0158	1	1
I_d	40	39, 40	6385	7857	6.72	44	23	39.55	29.9	2.8E7	100

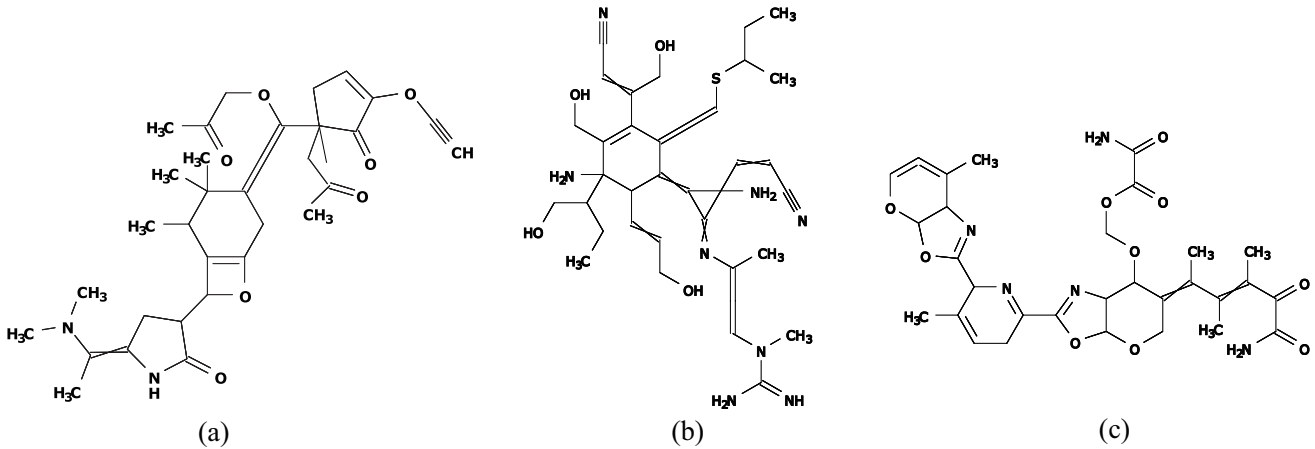


Figure 7: (a) \mathbb{C}^\dagger with $\eta(f(\mathbb{C}^\dagger)) = 132.827$ inferred from I_a with $(\underline{y}^*, \overline{y}^*) = (137, 140)$ of FP; (b) \mathbb{C}^\dagger with $\eta(f(\mathbb{C}^\dagger)) = 51.452$ inferred from I_b^2 with $(\underline{y}^*, \overline{y}^*) = (50, 52)$ of OPTR; and (c) \mathbb{C}^\dagger with $\eta(f(\mathbb{C}^\dagger)) = 44.557$ inferred from I_c with $(\underline{y}^*, \overline{y}^*) = (44, 45)$ of SFT.

restricted set of fringe-trees. From Tables 3 and 5, we observe that an instance with a large number of variables and constraints takes more running time than those with a smaller size in general. All

instances in this experiment are solved in a few seconds to around 150 seconds with our MILP formulation.

Stage 5. We executed Stage 5 to generate a more number of target chemical graphs \mathbb{C}^* , where we call a chemical graph \mathbb{C}^* a *chemical isomer* of a target chemical graph \mathbb{C}^\dagger of a topological specification σ if $f(\mathbb{C}^*) = f(\mathbb{C}^\dagger)$ and \mathbb{C}^* also satisfies the same topological specification σ . We computed chemical isomers \mathbb{C}^* of each target chemical graph \mathbb{C}^\dagger inferred in Stage 4. We execute an algorithm for generating chemical isomers of \mathbb{C}^\dagger up to 100 when the number of all chemical isomers exceeds 100. For this, we use a dynamic programming [24]. The algorithm first decomposes \mathbb{C}^\dagger into a set of acyclic chemical graphs, next replaces each acyclic chemical graph T with another acyclic chemical graph T' that admits the same feature vector as that of T and finally assembles the resulting acyclic chemical graphs into a chemical isomer \mathbb{C}^* of \mathbb{C}^\dagger . The algorithm can compute a lower bound on the total number of all chemical isomers \mathbb{C}^\dagger without generating all of them.

Tables 3 and 5 show the computational results of the experiment in Stage 5 for the five properties, where we denote the following:

- D-time: the running time (sec.) to execute the dynamic programming algorithm in Stage 5 to compute a lower bound on the number of all chemical isomers \mathbb{C}^* of \mathbb{C}^\dagger and generate all (or up to 100) chemical isomers \mathbb{C}^* ;
- C-LB: a lower bound on the number of all chemical isomers \mathbb{C}^* of \mathbb{C}^\dagger , where aEb means $a \times 10^b$; and
- $\#\mathbb{C}$: the number of all (or up to 100) chemical isomers \mathbb{C}^* of \mathbb{C}^\dagger generated in Stage 5.

From Tables 3 and 5, we observe the running time and the number of generated isomers in Stage 5. The chemical graph \mathbb{C}^\dagger in I_{b3} and I_d admits a large number of chemical isomers \mathbb{C}^* in some cases, where a lower bound C-LB on the number of chemical isomers is derived without generating all of them. For the other instances, the running time for generating up to 100 target chemical graphs in Stage 5 is less than one second. For some chemical graph \mathbb{C}^\dagger , no chemical isomer was found by our algorithm. This is because each acyclic chemical graph in the decomposition of \mathbb{C}^\dagger has no alternative acyclic chemical graph than the original one. For such an instance, we generate other desired chemical graphs by applying our new method of grid neighbor search.

Grid Neighbor Search. As a new building block of the framework of inferring chemical graphs, we conducted an experiment of applying our grid neighbor search to generate other solutions of an MILP in Stage 4. We select the MILP such that a solution \mathbb{C}^\dagger of the MILP admits at most two isomers \mathbb{C}^* in Stage 5; i.e., I_a with properties FP, OPTR and SFT; I_b^1 with properties FP and SFT; and I_c with properties FP, OPTR and SFT. In this experiment, we set $p_{\max} := 2$, $\delta := (0.1, 0.1)$, $r := (3, 3)$ and projection functions θ_1 and θ_2 to be linear prediction functions for properties solubility (SL) and lipophilicity (LP), respectively, constructed by Zhu et al. [24]. The number of non-center grids in the neighbor $N(r)$ is $7 \times 7 - 1 = 48$, where the center grid $z = (0, 0)$ is always feasible for the selected instances. For each instance, we check the feasibility of grids $z \in N(r)$ in a non-decreasing order of $\max_{p \in [1, p_{\max}]} |z(p)|$. For each feasible grid $z \in N(r)$, output a feasible solution \mathbb{C}_z^\dagger of the augmented MILP instance. We set a time limit for checking the feasibility of a grid to be 300 seconds, and we skip a grid when the corresponding MILP is not solved within the time limit. We also discard any grid $z \in N(r)$ without testing the feasibility of

z if we find an infeasible grid $z' \in N(r)$ with $z' \prec z$.

Tables 6 shows the computational results of the experiment in the grid neighbor search for the eight instances, where we denote the following:

- instance: a pair (I, π) of topological specification I and a property π in the tested instance;
- n : the number of non-hydrogen atoms in the tested instance;
- #feasible: the number of non-center grids in $N(r)$ that are found to be feasible during the search procedure;
- #solutions: the number of chemical graphs obtained from the feasible non-center grids in $N(r)$, where different feasible grids provide the same solutions and #feasible $>$ #solutions holds in such a case;
- #infeasible: the number of non-center grids in $N(r)$ that are found to be infeasible during the search procedure;
- #ignored: the number of non-center grids $z \in N(r)$ that are ignored due to an infeasible grid $z' \in N(r)$ with $z' \prec z$ during the search procedure;
- #time out: the number of non-center grids in $N(r)$ such that the time for feasibility check exceeds the time limit of 300 seconds during the search procedure;
- time: the average time for checking the feasibility of a non-center grid $z \in N(r)$ whose feasibility can be detected within the time limit.

Table 6: Results of Grid Neighbor Search.

instance	n	#feasible	#solutions	#infeasible	#ignored	#time out	time
(I_a, FP)	42	33	33	0	0	15	72.96
(I_a, OPTR)	47	30	30	1	2	15	44.00
(I_a, SFT)	41	45	45	0	0	3	11.91
(I_b^1, FP)	10	21	21	3	3	21	69.48
(I_b^1, SFT)	11	22	22	0	0	26	30.78
(I_c, FP)	50	33	33	0	0	15	71.84
(I_c, OPTR)	49	25	25	1	1	21	13.29
(I_c, SFT)	45	17	17	3	4	24	65.85

From Tables 6, we observe that our new method of grid neighbor search successfully infers other solutions than the chemical graphs \mathbb{C}^\dagger inferred by the standard Stage 4 even though Stage 5 could not find many chemical isomers \mathbb{C}^* of \mathbb{C}^\dagger . The branch-and-bound method for solving an MILP sometimes takes an extremely large execution time for the same size of instances. We introduce a time limit to bound an entire running time to skip such instances during an execution of testing the feasibility of grids in the neighbor $N(r)$. From Tables 6, we see that at least around a half number of grids in $N(r)$ were feasible and provided new solutions.

6 Concluding Remarks

In this paper, we designed a procedure for generating chemical graphs as a new building block in Stage 4 of the framework for inferring a desired chemical graph. The main task of Stage 4 is to find a feasible solution \mathbb{C}^\dagger of an MILP that represents a feature function and a topological specification. In the framework, isomers \mathbb{C}^* of \mathbb{C}^\dagger are generated in Stage 5 by a dynamic programming algorithm. However, the number of isomers of \mathbb{C}^\dagger is sometimes small. Our new procedure searches the neighbor of \mathbb{C}^\dagger in a search space defined with a set of linear functions. We divide the neighbor of \mathbb{C}^\dagger into subspaces and solve the MILP in Stage 4 for each subspace imposing a set of linear constraints that represents the subspace. From the results of our computational experiments, we observe that an additional number of solutions \mathbb{C}^* can be found in the neighbor of \mathbb{C}^\dagger by our new procedure.

References

- [1] Lo, Y-C., Rensi, S.E., Torng, W., Altman, R.B.: Machine learning in chemoinformatics and drug discovery. *Drug Discovery Today* **23**, 1538–1546 (2018)
- [2] Tetko, I.V., Engkvist, O.: From Big Data to Artificial Intelligence: chemoinformatics meets new challenges. *J. Cheminformatics* **12**, 74 (2020)
- [3] Ghasemi, F., Mehridehnavi, A., Pérez-Garrido, A., Pérez-Sánchez, H.: Neural network and deep-learning algorithms used in QSAR studies: merits and drawbacks. *Drug Discovery Today* **23**, 1784–1790 (2018)
- [4] Miyao, T., Kaneko, H., Funatsu, K.: Inverse QSPR/QSAR analysis for chemical structure generation (from y to x). *J. Chem. Inf. Model.* **56**, 286–299 (2016)
- [5] Ikebata, H., Hongo, K., Isomura, T., Maezono, R., Yoshida, R.: Bayesian molecular design with a chemical language model. *J. Comput. Aided Mol. Des.* **31**, 379–391 (2017)
- [6] Rupakheti, C., Virshup, A., Yang, W., Beratan, D.N.: Strategy to discover diverse optimal molecules in the small molecule universe. *J. Chem. Inf. Model.* **55**, 529–537 (2015)
- [7] Bohacek, R.S., McMartin, C., Guida, W.C.: The art and practice of structure-based drug design: A molecular modeling perspective. *Med. Res. Rev.* **16**, 3–50 (1996)
- [8] Akutsu, T., Fukagawa, D., Jansson, J., Sadakane, K.: Inferring a graph from path frequency. *Discrete Appl. Math.* **160**, 10–11, 1416–1428 (2012)
- [9] Kipf, T. N., Welling, M.: Semi-supervised classification with graph convolutional networks, arXiv:1609.02907 (2016)
- [10] Gómez-Bombarelli, R., Wei, J.N., Duvenaud, D., Hernández-Lobato, J.M., Sánchez-Lengeling, B., Sheberla, D., Aguilera-Iparraguirre, J., Hirzel, T.D., Adams, R.P., Aspuru-Guzik, A.: Automatic chemical design using a data-driven continuous representation of molecules. *ACS Cent. Sci.* **4**, 268–276 (2018)

- [11] Segler, M.H.S., Kogej, T., Tyrchan, C., Waller, M.P.: Generating focused molecule libraries for drug discovery with recurrent neural networks. *ACS Cent. Sci.* **4**, 120–131 (2017)
- [12] Yang, X., Zhang, J., Yoshizoe, K., Terayama, K., Tsuda, K.: ChemTS: an efficient python library for de novo molecular generation. *STAM* **18**, 972–976 (2017)
- [13] Kusner, M.J., Paige, B., Hernández-Lobato, J.M.: Grammar variational autoencoder. *Proc. of the 34th International Conference on Machine Learning-Volume 70*, 1945–1954 (2017)
- [14] De Cao, N., Kipf, T.: MolGAN: An implicit generative model for small molecular graphs. *arXiv:1805.11973* (2018)
- [15] Madhawa, K., Ishiguro, K., Nakago, K., Abe, M.: GraphNVP: an invertible flow model for generating molecular graphs. *arXiv:1905.11600* (2019)
- [16] Shi, C., Xu, M., Zhu, Z., Zhang, W., Zhang, M., Tang, J.: GraphAF: a flow-based autoregressive model for molecular graph generation. *arXiv:2001.09382* (2020)
- [17] Akutsu, T., Nagamochi, H.: A mixed integer linear programming formulation to artificial neural networks. *Proc. of the 2nd Int. Conf. on Information Science and Systems*, 215–220 (2019)
- [18] Azam, N. A., Chiewvanichakorn, R., Zhang, F., Shurbevski, A., Nagamochi, H., Akutsu, T.: A method for the inverse QSAR/QSPR based on artificial neural networks and mixed integer linear programming. *Proc. of the 13th International Joint Conference on Biomedical Engineering Systems and Technologies – Volume 3: BIOINFORMATICS*, 101–108 (2020)
- [19] Azam, N. A., Zhu, J., Sun, Y., Shi, Y., Shurbevski, A., Zhao, L., Nagamochi, H., Akutsu, T.: A novel method for inference of acyclic chemical compounds with bounded branch-height based on artificial neural networks and integer programming. *Algorithms for Molecular Biology*, **16**, 18 (2021)
- [20] Zhu, J., Wang, C., Shurbevski, A., Nagamochi, H., Akutsu, T.: A novel method for inference of chemical compounds of cycle index two with desired properties based on artificial neural networks and integer programming. *Algorithms* **13**, 5, 124 (2020)
- [21] Zhu, J., Azam, N. A., Zhang, F., Shurbevski, A., Haraguchi, K., Zhao, L., Nagamochi, H., Akutsu, T.: A novel method for inferring of chemical compounds with prescribed topological substructures based on integer programming. *IEEE/ACM Trans. Comput. Biol. Bioinform* (submitted).
- [22] Shi, Y., Zhu, J., Azam, N. A., Haraguchi, K., Zhao, L., Nagamochi, H., Akutsu, T.: An inverse QSAR method based on a two-layered model and integer programming. *International Journal of Molecular Sciences*. **22**, 2847 (2021)
- [23] Tanaka, K., Zhu, J., Azam, N. A., Haraguchi, K., Zhao, L., Nagamochi, H., Akutsu, T.: An inverse QSAR method based on decision tree and integer programming. *The 17th International Conference on Intelligent Computing*, August 12-15, 2021, in Shenzhen, China, In:

- Huang D.S., Jo K.H., Li J., Gribova V., Hussain A. (eds) Intelligent Computing Theories and Application, ICIC 2021, Lecture Notes in Computer Science, vol. 12837. Springer, Cham.
- [24] Zhu, J., Azam, N. A., Haraguchi, K., Zhao, L., Nagamochi, H., Akutsu, T.: A method for molecular design based on linear regression and integer programming. 12th International Conference on Bioscience, Biochemistry and Bioinformatics (ICBBB 2022), Tokyo, Japan during January 7-10, 2022 (to appear)
- [25] Ido, R., Cao, S., Zhu, J., Azam, N. A., Haraguchi, K., Zhao, L., Nagamochi, H., Akutsu, T.: A method for inferring polymers based on linear regression and integer programming. arXiv: (to be registered) (2021)
- [26] Annotations from HSDB (on pubchem): <https://pubchem.ncbi.nlm.nih.gov/>
- [27] Jalali-Heravi, M., Fatemi, M.: Artificial neural network modeling of Kovats retention indices for noncyclic and monocyclic terpenes (2001) [https://doi.org/10.1016/S0021-9673\(00\)01274-7/](https://doi.org/10.1016/S0021-9673(00)01274-7/)
- [28] Roy, K., Saha, A.: Comparative QSPR studies with molecular connectivity, molecular negentropy and TAU indices (2003) <https://doi.org/10.1007/s00894-003-0135-z/>
- [29] QM9 at MoleculeNet: <http://moleculenet.ai>
- [30] Goussard, V., Duprat, F., Gerbaud, V., Ploix, J.-J., Dreyfus, G., Nardello-Rataj, V., Aubry, J.-M.: Predicting the surface tension of liquids: comparison of four modeling approaches and application to cosmetic oils, *J. Chem. Inf. Model.*, 57, 12, 2986–2995 (2017) <https://pubs.acs.org/doi/full/10.1021/acs.jcim.7b00512>
- [31] Goussard, V., François Duprat F., Ploix, J.-L., Dreyfus, G., Nardello-Rataj, V., Aubry, J.-M.: A new machine-learning tool for fast estimation of liquid viscosity. application to cosmetic oils. *J. Chem. Inf. Model.*, 60, 4, 2012–2023 (2020) <https://pubs.acs.org/doi/10.1021/acs.jcim.0c00083>
- [32] Naef, R.: Calculation of the isobaric heat capacities of the liquid and solid phase of organic compounds at and around 298.15 K based on their “true” molecular volume. *Molecules*, 24 (8) (2019), <https://www.mdpi.com/1420-3049/24/8/1626/>
- [33] https://figshare.com/articles/dataset/Lipophilicity_Dataset_-_logD7_4_of_1_130_Compounds/5596750/1
- [34] ESOL at MoleculeNet: <http://moleculenet.ai/datasets-1>
- [35] Bicerano, J.: Prediction of Polymer Properties. 3rd Edition, Revised and Expanded. CRC Press (2002)

Appendix

A A Full Description of Descriptors

Associated with the two functions α and β in a chemical graph $\mathbb{C} = (H, \alpha, \beta)$, we introduce functions $ac : V(E) \rightarrow (\Lambda \setminus \{\text{H}\}) \times (\Lambda \setminus \{\text{H}\}) \times [1, 3]$, $cs : V(E) \rightarrow (\Lambda \setminus \{\text{H}\}) \times [1, 6]$ and $ec : V(E) \rightarrow ((\Lambda \setminus \{\text{H}\}) \times [1, 6]) \times ((\Lambda \setminus \{\text{H}\}) \times [1, 6]) \times [1, 3]$ in the following.

To represent a feature of the exterior of \mathbb{C} , a chemical rooted tree in $\mathcal{T}(\mathbb{C})$ is called a *fringe-configuration* of \mathbb{C} .

We also represent leaf-edges in the exterior of \mathbb{C} . For a leaf-edge $uv \in E(\langle \mathbb{C} \rangle)$ with $\deg_{\langle \mathbb{C} \rangle}(u) = 1$, we define the *adjacency-configuration* of e to be an ordered tuple $(\alpha(u), \alpha(v), \beta(uv))$. Define

$$\Gamma_{ac}^{\text{lf}} \triangleq \{(\mathbf{a}, \mathbf{b}, m) \mid \mathbf{a}, \mathbf{b} \in \Lambda, m \in [1, \min\{\text{val}(\mathbf{a}), \text{val}(\mathbf{b})\}]\}$$

as a set of possible adjacency-configurations for leaf-edges.

To represent a feature of an interior-vertex $v \in V^{\text{int}}(\mathbb{C})$ such that $\alpha(v) = \mathbf{a}$ and $\deg_{\langle \mathbb{C} \rangle}(v) = d$ (i.e., the number of non-hydrogen atoms adjacent to v is d) in a chemical graph $\mathbb{C} = (H, \alpha, \beta)$, we use a pair $(\mathbf{a}, d) \in (\Lambda \setminus \{\text{H}\}) \times [1, 4]$, which we call the *chemical symbol* $cs(v)$ of the vertex v . We treat (\mathbf{a}, d) as a single symbol \mathbf{ad} , and define Λ_{dg} to be the set of all chemical symbols $\mu = \mathbf{ad} \in (\Lambda \setminus \{\text{H}\}) \times [1, 4]$.

We define a method for featuring interior-edges as follows. Let $e = uv \in E^{\text{int}}(\mathbb{C})$ be an interior-edge $e = uv \in E^{\text{int}}(\mathbb{C})$ such that $\alpha(u) = \mathbf{a}$, $\alpha(v) = \mathbf{b}$ and $\beta(e) = m$ in a chemical graph $\mathbb{C} = (H, \alpha, \beta)$. To feature this edge e , we use a tuple $(\mathbf{a}, \mathbf{b}, m) \in (\Lambda \setminus \{\text{H}\}) \times (\Lambda \setminus \{\text{H}\}) \times [1, 3]$, which we call the *adjacency-configuration* $ac(e)$ of the edge e . We introduce a total order $<$ over the elements in Λ to distinguish between $(\mathbf{a}, \mathbf{b}, m)$ and $(\mathbf{b}, \mathbf{a}, m)$ ($\mathbf{a} \neq \mathbf{b}$) notationally. For a tuple $\nu = (\mathbf{a}, \mathbf{b}, m)$, let $\bar{\nu}$ denote the tuple $(\mathbf{b}, \mathbf{a}, m)$.

Let $e = uv \in E^{\text{int}}(\mathbb{C})$ be an interior-edge $e = uv \in E^{\text{int}}(\mathbb{C})$ such that $cs(u) = \mu$, $cs(v) = \mu'$ and $\beta(e) = m$ in a chemical graph $\mathbb{C} = (H, \alpha, \beta)$. To feature this edge e , we use a tuple $(\mu, \mu', m) \in \Lambda_{\text{dg}} \times \Lambda_{\text{dg}} \times [1, 3]$, which we call the *edge-configuration* $ec(e)$ of the edge e . We introduce a total order $<$ over the elements in Λ_{dg} to distinguish between (μ, μ', m) and (μ', μ, m) ($\mu \neq \mu'$) notationally. For a tuple $\gamma = (\mu, \mu', m)$, let $\bar{\gamma}$ denote the tuple (μ', μ, m) .

Let π be a chemical property for which we will construct a prediction function η from a feature vector $f(\mathbb{C})$ of a chemical graph \mathbb{C} to a predicted value $y \in \mathbb{R}$ for the chemical property of \mathbb{C} .

We first choose a set Λ of chemical elements and then collect a data set D_π of chemical compounds C whose chemical elements belong to Λ , where we regard D_π as a set of chemical graphs \mathbb{C} that represent the chemical compounds C in D_π . To define the interior/exterior of chemical graphs $\mathbb{C} \in D_\pi$, we next choose a branch-parameter ρ , where we recommend $\rho = 2$.

Let $\Lambda^{\text{int}}(D_\pi) \subseteq \Lambda$ (resp., $\Lambda^{\text{ex}}(D_\pi) \subseteq \Lambda$) denote the set of chemical elements used in the set $V^{\text{int}}(\mathbb{C})$ of interior-vertices (resp., the set $V^{\text{ex}}(\mathbb{C})$ of exterior-vertices) of \mathbb{C} over all chemical graphs $\mathbb{C} \in D_\pi$, and $\Gamma^{\text{int}}(D_\pi)$ denote the set of edge-configurations used in the set $E^{\text{int}}(\mathbb{C})$ of interior-edges in \mathbb{C} over all chemical graphs $\mathbb{C} \in D_\pi$. Let $\mathcal{F}(D_\pi)$ denote the set of chemical rooted trees ψ r-isomorphic to a chemical rooted tree in $\mathcal{T}(\mathbb{C})$ over all chemical graphs $\mathbb{C} \in D_\pi$, where possibly a chemical rooted tree $\psi \in \mathcal{F}(D_\pi)$ consists of a single chemical element $\mathbf{a} \in \Lambda \setminus \{\text{H}\}$.

We define an integer encoding of a finite set A of elements to be a bijection $\sigma : A \rightarrow [1, |A|]$, where we denote by $[A]$ the set $[1, |A|]$ of integers. Introduce an integer coding of each of the sets $\Lambda^{\text{int}}(D_\pi)$, $\Lambda^{\text{ex}}(D_\pi)$, $\Gamma^{\text{int}}(D_\pi)$ and $\mathcal{F}(D_\pi)$. Let $[\mathbf{a}]^{\text{int}}$ (resp., $[\mathbf{a}]^{\text{ex}}$) denote the coded integer of an element $\mathbf{a} \in \Lambda^{\text{int}}(D_\pi)$ (resp., $\mathbf{a} \in \Lambda^{\text{ex}}(D_\pi)$), $[\gamma]$ denote the coded integer of an element γ in $\Gamma^{\text{int}}(D_\pi)$ and $[\psi]$ denote an element ψ in $\mathcal{F}(D_\pi)$.

Over 99% of chemical compounds \mathbb{C} with up to 100 non-hydrogen atoms in PubChem have degree at most 4 in the hydrogen-suppressed graph $\langle \mathbb{C} \rangle$ [19]. We assume that a chemical graph \mathbb{C} treated in this paper satisfies $\deg_{\langle \mathbb{C} \rangle}(v) \leq 4$ in the hydrogen-suppressed graph $\langle \mathbb{C} \rangle$.

In our model, we use an integer $\text{mass}^*(\mathbf{a}) = \lfloor 10 \cdot \text{mass}(\mathbf{a}) \rfloor$, for each $\mathbf{a} \in \Lambda$.

We define the *feature vector* $f(\mathbb{C})$ of a chemical graph $\mathbb{C} = (H, \alpha, \beta) \in D_\pi$ to be a vector that consists of the following non-negative integer descriptors $\text{dcp}_i(\mathbb{C})$, $i \in [1, K]$, where $K = 14 + |\Lambda^{\text{int}}(D_\pi)| + |\Lambda^{\text{ex}}(D_\pi)| + |\Gamma^{\text{int}}(D_\pi)| + |\mathcal{F}(D_\pi)| + |\Gamma_{\text{ac}}^{\text{lf}}|$.

1. $\text{dcp}_1(\mathbb{C})$: the number $|V(H)| - |V_{\text{H}}|$ of non-hydrogen atoms in \mathbb{C} .
2. $\text{dcp}_2(\mathbb{C})$: the rank $r(\mathbb{C})$ of \mathbb{C} .
3. $\text{dcp}_3(\mathbb{C})$: the number $|V^{\text{int}}(\mathbb{C})|$ of interior-vertices in \mathbb{C} .
4. $\text{dcp}_4(\mathbb{C})$: the average $\overline{\text{ms}}(\mathbb{C})$ of mass^* over all atoms in \mathbb{C} ;
i.e., $\overline{\text{ms}}(\mathbb{C}) \triangleq \frac{1}{|V(H)|} \sum_{v \in V(H)} \text{mass}^*(\alpha(v))$.
5. $\text{dcp}_i(\mathbb{C})$, $i = 4 + d$, $d \in [1, 4]$: the number $\text{dg}_d^{\text{H}}(\mathbb{C})$ of non-hydrogen vertices $v \in V(H) \setminus V_{\text{H}}$ of degree $\deg_{\langle \mathbb{C} \rangle}(v) = d$ in the hydrogen-suppressed chemical graph $\langle \mathbb{C} \rangle$.
6. $\text{dcp}_i(\mathbb{C})$, $i = 8 + d$, $d \in [1, 4]$: the number $\text{dg}_d^{\text{int}}(\mathbb{C})$ of interior-vertices of interior-degree $\deg_{\mathbb{C}^{\text{int}}}(v) = d$ in the interior $\mathbb{C}^{\text{int}} = (V^{\text{int}}(\mathbb{C}), E^{\text{int}}(\mathbb{C}))$ of \mathbb{C} .
7. $\text{dcp}_i(\mathbb{C})$, $i = 12 + m$, $m \in [2, 3]$: the number $\text{bd}_m^{\text{int}}(\mathbb{C})$ of interior-edges with bond multiplicity m in \mathbb{C} ; i.e., $\text{bd}_m^{\text{int}}(\mathbb{C}) \triangleq \{e \in E^{\text{int}}(\mathbb{C}) \mid \beta(e) = m\}$.
8. $\text{dcp}_i(\mathbb{C})$, $i = 14 + [\mathbf{a}]^{\text{int}}$, $\mathbf{a} \in \Lambda^{\text{int}}(D_\pi)$: the frequency $\text{na}_{\mathbf{a}}^{\text{int}}(\mathbb{C}) = |V_{\mathbf{a}}(\mathbb{C}) \cap V^{\text{int}}(\mathbb{C})|$ of chemical element \mathbf{a} in the set $V^{\text{int}}(\mathbb{C})$ of interior-vertices in \mathbb{C} .
9. $\text{dcp}_i(\mathbb{C})$, $i = 14 + |\Lambda^{\text{int}}(D_\pi)| + [\mathbf{a}]^{\text{ex}}$, $\mathbf{a} \in \Lambda^{\text{ex}}(D_\pi)$: the frequency $\text{na}_{\mathbf{a}}^{\text{ex}}(\mathbb{C}) = |V_{\mathbf{a}}(\mathbb{C}) \cap V^{\text{ex}}(\mathbb{C})|$ of chemical element \mathbf{a} in the set $V^{\text{ex}}(\mathbb{C})$ of exterior-vertices in \mathbb{C} .
10. $\text{dcp}_i(\mathbb{C})$, $i = 14 + |\Lambda^{\text{int}}(D_\pi)| + |\Lambda^{\text{ex}}(D_\pi)| + [\gamma]$, $\gamma \in \Gamma^{\text{int}}(D_\pi)$: the frequency $\text{ec}_\gamma(\mathbb{C})$ of edge-configuration γ in the set $E^{\text{int}}(\mathbb{C})$ of interior-edges in \mathbb{C} .
11. $\text{dcp}_i(\mathbb{C})$, $i = 14 + |\Lambda^{\text{int}}(D_\pi)| + |\Lambda^{\text{ex}}(D_\pi)| + |\Gamma^{\text{int}}(D_\pi)| + [\psi]$, $\psi \in \mathcal{F}(D_\pi)$: the frequency $\text{fc}_\psi(\mathbb{C})$ of fringe-configuration ψ in the set of ρ -fringe-trees in \mathbb{C} .
12. $\text{dcp}_i(\mathbb{C})$, $i = 14 + |\Lambda^{\text{int}}(D_\pi)| + |\Lambda^{\text{ex}}(D_\pi)| + |\Gamma^{\text{int}}(D_\pi)| + |\mathcal{F}(D_\pi)| + [\nu]$, $\nu \in \Gamma_{\text{ac}}^{\text{lf}}$: the frequency $\text{ac}_\nu^{\text{lf}}(\mathbb{C})$ of adjacency-configuration ν in the set of leaf-edges in $\langle \mathbb{C} \rangle$.

B Specifying Target Chemical Graphs

Given a prediction function η and a target value $y^* \in \mathbb{R}$, we call a chemical graph \mathbb{C}^* such that $\eta(x^*) = y^*$ for the feature vector $x^* = f(\mathbb{C}^*)$ a *target chemical graph*. This section presents a set of rules for specifying topological substructure of a target chemical graph in a flexible way in Stage 4.

We first describe how to reduce a chemical graph $\mathbb{C} = (H, \alpha, \beta)$ into an abstract form based on which our specification rules will be defined. To illustrate the reduction process, we use the chemical graph $\mathbb{C} = (H, \alpha, \beta)$ such that $\langle \mathbb{C} \rangle$ is given in Figure 2.

R1 Removal of all ρ -fringe-trees: The interior $H^{\text{int}} = (V^{\text{int}}(\mathbb{C}), E^{\text{int}}(\mathbb{C}))$ of \mathbb{C} is obtained by removing the non-root vertices of each ρ -fringe-trees $\mathbb{C}[u] \in \mathcal{T}(\mathbb{C}), u \in V^{\text{int}}(\mathbb{C})$. Figure 8 illustrates the interior H^{int} of chemical graph \mathbb{C} with $\rho = 2$ in Figure 2.

R2 Removal of some leaf paths: We call a u, v -path Q in H^{int} a *leaf path* if vertex v is a leaf-vertex of H^{int} and the degree of each internal vertex of Q in H^{int} is 2, where we regard that Q is rooted at vertex u . A connected subgraph S of the interior H^{int} of \mathbb{C} is called a *cyclical-base* if S is obtained from H by removing the vertices in $V(Q_u) \setminus \{u\}, u \in X$ for a subset X of interior-vertices and a set $\{Q_u \mid u \in X\}$ of leaf u, v -paths Q_u such that no two paths Q_u and $Q_{u'}$ share a vertex. Figure 9(a) illustrates a cyclical-base $S = H^{\text{int}} - \bigcup_{u \in X} (V(Q_u) \setminus \{u\})$ of the interior H^{int} for a set $\{Q_{u_5} = (u_5, u_{24}), Q_{u_{18}} = (u_{18}, u_{25}, u_{26}, u_{27}), Q_{u_{22}} = (u_{22}, u_{28})\}$ of leaf paths in Figure 8.

R3 Contraction of some pure paths: A path in S is called *pure* if each internal vertex of the path is of degree 2. Choose a set \mathcal{P} of several pure paths in S so that no two paths share vertices except for their end-vertices. A graph S' is called a *contraction* of a graph S (with respect to \mathcal{P}) if S' is obtained from S by replacing each pure u, v -path with a single edge $a = uv$, where S' may contain multiple edges between the same pair of adjacent vertices. Figure 9(b) illustrates a contraction S' obtained from the chemical graph S by contracting each uv -path $P_a \in \mathcal{P}$ into a new edge $a = uv$, where $a_1 = u_1u_2, a_2 = u_1u_3, a_3 = u_4u_7, a_4 = u_{10}u_{11}$ and $a_5 = u_{11}u_{12}$ and $\mathcal{P} = \{P_{a_1} = (u_1, u_{13}, u_2), P_{a_2} = (u_1, u_{14}, u_3), P_{a_3} = (u_4, u_{15}, u_{16}, u_7), P_{a_4} = (u_{10}, u_{17}, u_{18}, u_{19}, u_{11}), P_{a_5} = (u_{11}, u_{20}, u_{21}, u_{22}, u_{12})\}$ of pure paths in Figure 9(a).

We will define a set of rules so that a chemical graph can be obtained from a graph (called a seed graph in the next section) by applying processes R3 to R1 in a reverse way. We specify topological substructures of a target chemical graph with a tuple $(G_C, \sigma_{\text{int}}, \sigma_{\text{ce}})$ called a *target specification* defined under the set of the following rules.

Seed Graph

A *seed graph* $G_C = (V_C, E_C)$ is defined to be a graph (possibly with multiple edges) such that the edge set E_C consists of four sets $E_{(\geq 2)}, E_{(\geq 1)}, E_{(0/1)}$ and $E_{(=1)}$, where each of them can be empty. A seed graph plays a role of the most abstract form S' in R3. Figure 4(a) illustrates an example of a seed graph G_C with $r(G_C) = 5$, where $V_C = \{u_1, u_2, \dots, u_{12}, u_{23}\}$, $E_{(\geq 2)} = \{a_1, a_2, \dots, a_5\}$, $E_{(\geq 1)} = \{a_6\}$, $E_{(0/1)} = \{a_7\}$ and $E_{(=1)} = \{a_8, a_9, \dots, a_{16}\}$.

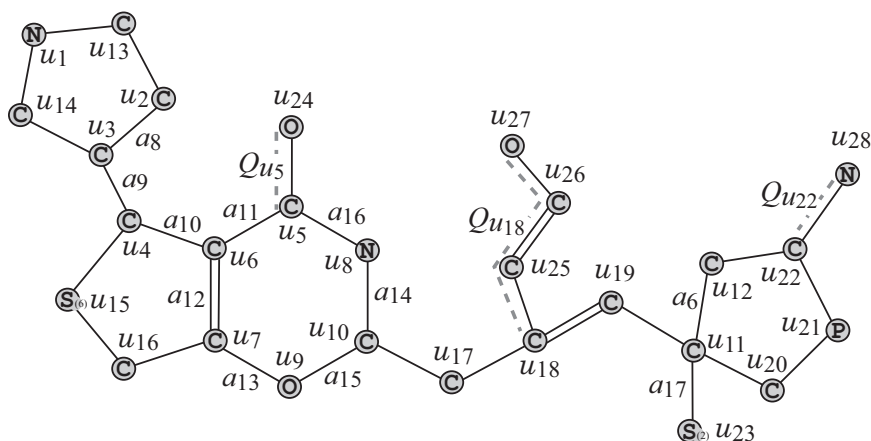
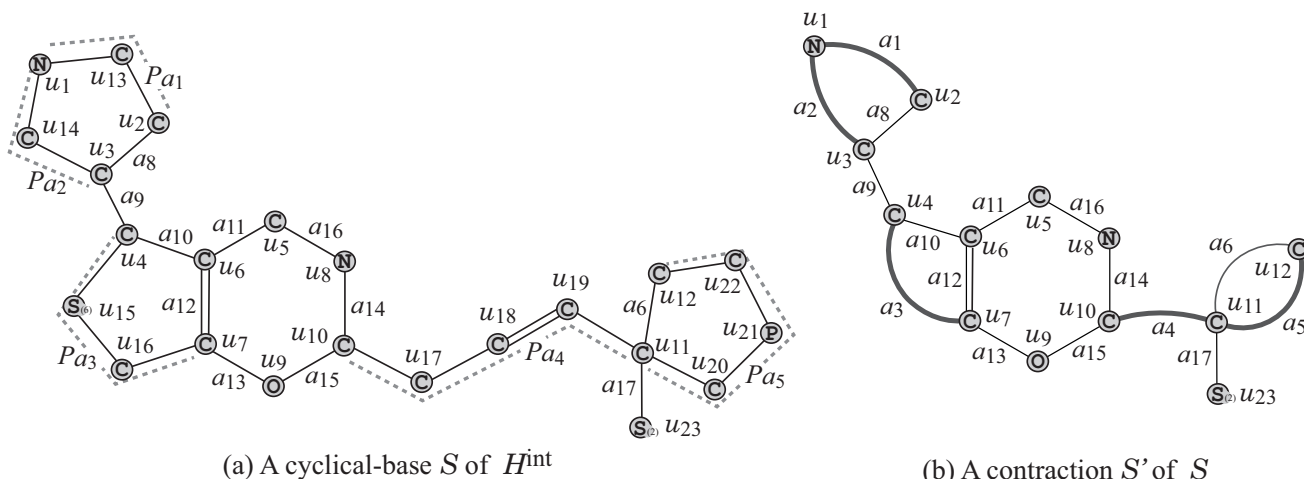


Figure 8: The interior H^{int} of chemical graph \mathbb{C} with $\langle \mathbb{C} \rangle$ in Figure 2 for $\rho = 2$.



(a) A cyclical-base S of H^{int}

(b) A contraction S' of S

Figure 9: (a) A cyclical-base $S = H^{\text{int}} - \bigcup_{u \in \{u_5, u_{18}, u_{22}\}} (V(Q_u) \setminus \{u\})$ of the interior H^{int} in Figure 8; (b) A contraction S' of S for a pure path set $\mathcal{P} = \{P_{a_1}, P_{a_2}, \dots, P_{a_5}\}$ in (a), where a new edge obtained by contracting a pure path is depicted with a thick line.

A *subdivision* S of $G_{\mathbb{C}}$ is a graph constructed from a seed graph $G_{\mathbb{C}}$ according to the following rules:

- Each edge $e = uv \in E_{(\geq 2)}$ is replaced with a u, v -path P_e of length at least 2;
- Each edge $e = uv \in E_{(\geq 1)}$ is replaced with a u, v -path P_e of length at least 1 (equivalently e is directly used or replaced with a u, v -path P_e of length at least 2);
- Each edge $e \in E_{(0/1)}$ is either used or discarded, where $E_{(0/1)}$ is required to be chosen as a non-separating edge subset of $E(G_{\mathbb{C}})$ since otherwise the connectivity of a final chemical graph \mathbb{C} is not guaranteed; $r(\mathbb{C}) = r(G_{\mathbb{C}}) - |E'|$ holds for a subset $E' \subseteq E_{(0/1)}$ of edges discarded in a final chemical graph \mathbb{C} ; and

- Each edge $e \in E_{(=1)}$ is always used directly.

We allow a possible elimination of edges in $E_{(0/1)}$ as an optional rule in constructing a target chemical graph from a seed graph, even though such an operation has not been included in the process R3. A subdivision S plays a role of a cyclical-base in R2. A target chemical graph $\mathbb{C} = (H, \alpha, \beta)$ will contain S as a subgraph of the interior H^{int} of \mathbb{C} .

Interior-specification

A graph H^* that serves as the interior H^{int} of a target chemical graph \mathbb{C} will be constructed as follows. First construct a subdivision S of a seed graph G_C by replacing each edge $e = uu' \in E_{(\geq 2)} \cup E_{(\geq 1)}$ with a pure u, u' -path P_e . Next construct a supergraph H^* of S by attaching a leaf path Q_v at each vertex $v \in V_C$ or at an internal vertex $v \in V(P_e) \setminus \{u, u'\}$ of each pure u, u' -path P_e for some edge $e = uu' \in E_{(\geq 2)} \cup E_{(\geq 1)}$, where possibly $Q_v = (v), E(Q_v) = \emptyset$ (i.e., we do not attach any new edges to v). We introduce the following rules for specifying the size of H^* , the length $|E(P_e)|$ of a pure path P_e , the length $|E(Q_v)|$ of a leaf path Q_v , the number of leaf paths Q_v and a bond-multiplicity of each interior-edge, where we call the set of prescribed constants an *interior-specification* σ_{int} :

- Lower and upper bounds $n_{\text{LB}}^{\text{int}}, n_{\text{UB}}^{\text{int}} \in \mathbb{Z}_+$ on the number of interior-vertices of a target chemical graph \mathbb{C} .
- For each edge $e = uu' \in E_{(\geq 2)} \cup E_{(\geq 1)}$,
 - a lower bound $\ell_{\text{LB}}(e)$ and an upper bound $\ell_{\text{UB}}(e)$ on the length $|E(P_e)|$ of a pure u, u' -path P_e . (For a notational convenience, set $\ell_{\text{LB}}(e) := 0, \ell_{\text{UB}}(e) := 1, e \in E_{(0/1)}$ and $\ell_{\text{LB}}(e) := 1, \ell_{\text{UB}}(e) := 1, e \in E_{(=1)}$.)
 - a lower bound $\text{bl}_{\text{LB}}(e)$ and an upper bound $\text{bl}_{\text{UB}}(e)$ on the number of leaf paths Q_v attached at internal vertices v of a pure u, u' -path P_e .
 - a lower bound $\text{ch}_{\text{LB}}(e)$ and an upper bound $\text{ch}_{\text{UB}}(e)$ on the maximum length $|E(Q_v)|$ of a leaf path Q_v attached at an internal vertex $v \in V(P_e) \setminus \{u, u'\}$ of a pure u, u' -path P_e .
- For each vertex $v \in V_C$,
 - a lower bound $\text{ch}_{\text{LB}}(v)$ and an upper bound $\text{ch}_{\text{UB}}(v)$ on the number of leaf paths Q_v attached to v , where $0 \leq \text{ch}_{\text{LB}}(v) \leq \text{ch}_{\text{UB}}(v) \leq 1$.
 - a lower bound $\text{ch}_{\text{LB}}(v)$ and an upper bound $\text{ch}_{\text{UB}}(v)$ on the length $|E(Q_v)|$ of a leaf path Q_v attached to v .
- For each edge $e = uu' \in E_C$, a lower bound $\text{bd}_{m,\text{LB}}(e)$ and an upper bound $\text{bd}_{m,\text{UB}}(e)$ on the number of edges with bond-multiplicity $m \in [2, 3]$ in u, u' -path P_e , where we regard $P_e, e \in E_{(0/1)} \cup E_{(=1)}$ as single edge e .

We call a graph H^* that satisfies an interior-specification σ_{int} a σ_{int} -*extension* of G_C , where the bond-multiplicity of each edge has been determined.

Table 7: Example 1 of an interior-specification σ_{int} .

$n_{\text{LB}}^{\text{int}} = 20$	$n_{\text{UB}}^{\text{int}} = 28$					
	a_1	a_2	a_3	a_4	a_5	a_6
$\ell_{\text{LB}}(a_i)$	2	2	2	3	2	1
$\ell_{\text{UB}}(a_i)$	3	4	3	5	4	4
$\text{bl}_{\text{LB}}(a_i)$	0	0	0	1	1	0
$\text{bl}_{\text{UB}}(a_i)$	1	1	0	2	1	0
$\text{ch}_{\text{LB}}(a_i)$	0	1	0	4	3	0
$\text{ch}_{\text{UB}}(a_i)$	3	3	1	6	5	2

	u_1	u_2	u_3	u_4	u_5	u_6	u_7	u_8	u_9	u_{10}	u_{11}	u_{12}	u_{23}
$\text{bl}_{\text{LB}}(u_i)$	0	0	0	0	0	0	0	0	0	0	0	0	0
$\text{bl}_{\text{UB}}(u_i)$	1	1	1	1	1	0	0	0	0	0	0	0	0
$\text{ch}_{\text{LB}}(u_i)$	0	0	0	0	1	0	0	0	0	0	0	0	0
$\text{ch}_{\text{UB}}(u_i)$	1	0	0	0	3	0	1	1	0	1	2	4	1

	a_1	a_2	a_3	a_4	a_5	a_6	a_7	a_8	a_9	a_{10}	a_{11}	a_{12}	a_{13}	a_{14}	a_{15}	a_{16}	a_{17}
$\text{bd}_{2,\text{LB}}(a_i)$	0	0	0	1	0	0	0	0	0	0	0	1	0	0	0	0	0
$\text{bd}_{2,\text{UB}}(a_i)$	1	1	0	2	2	0	0	0	0	0	0	1	0	0	0	0	0
$\text{bd}_{3,\text{LB}}(a_i)$	0	0	0	0	0	0	0	0	0	0	0	0	0	0	0	0	0
$\text{bd}_{3,\text{UB}}(a_i)$	0	0	0	0	1	0	0	0	0	0	0	0	0	0	0	0	0

Table 7 shows an example of an interior-specification σ_{int} to the seed graph G_C in Figure 4.

Figure 10 illustrates an example of an σ_{int} -extension H^* of seed graph G_C in Figure 4 under the interior-specification σ_{int} in Table 7.

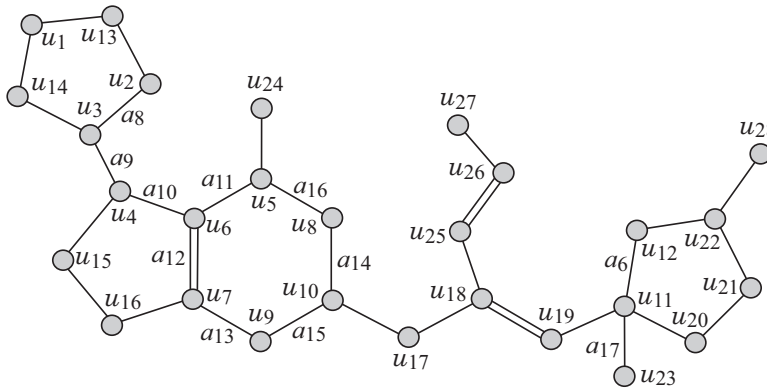


Figure 10: An illustration of a graph H^* that is obtained from the seed graph G_C in Figure 4 under the interior-specification σ_{int} in Table 7, where the vertices newly introduced by pure paths P_{a_i} and leaf paths Q_{v_i} are depicted with white squares and circles, respectively.

Chemical-specification

Let H^* be a graph that serves as the interior H^{int} of a target chemical graph \mathbb{C} , where the bond-multiplicity of each edge in H^* has been determined. Finally we introduce a set of rules for constructing a target chemical graph \mathbb{C} from H^* by choosing a chemical element $\mathbf{a} \in \Lambda$ and assigning a ρ -fringe-tree ψ to each interior-vertex $v \in V^{\text{int}}$. We introduce the following rules for specifying the size of \mathbb{C} , a set of chemical rooted trees that are allowed to use as ρ -fringe-trees and lower and upper bounds on the frequency of a chemical element, a chemical symbol, and an edge-configuration, where we call the set of prescribed constants a *chemical specification* σ_{ce} :

- Lower and upper bounds $n_{\text{LB}}, n^* \in \mathbb{Z}_+$ on the number of vertices, where $n_{\text{LB}}^{\text{int}} \leq n_{\text{LB}} \leq n^*$.
- Subsets $\mathcal{F}(v) \subseteq \mathcal{F}(D_\pi), v \in V_{\mathbb{C}}$ and $\mathcal{F}_E \subseteq \mathcal{F}(D_\pi)$ of chemical rooted trees ψ with $\text{ht}(\langle \psi \rangle) \leq \rho$, where we require that every ρ -fringe-tree $\mathbb{C}[v]$ rooted at a vertex $v \in V_{\mathbb{C}}$ (resp., at an internal vertex v not in $V_{\mathbb{C}}$) in \mathbb{C} belongs to $\mathcal{F}(v)$ (resp., \mathcal{F}_E). Let $\mathcal{F}^* := \mathcal{F}_E \cup \bigcup_{v \in V_{\mathbb{C}}} \mathcal{F}(v)$ and Λ^{ex} denote the set of chemical elements assigned to non-root vertices over all chemical rooted trees in \mathcal{F}^* .
- A subset $\Lambda^{\text{int}} \subseteq \Lambda^{\text{int}}(D_\pi)$, where we require that every chemical element $\alpha(v)$ assigned to an interior-vertex v in \mathbb{C} belongs to Λ^{int} . Let $\Lambda := \Lambda^{\text{int}} \cup \Lambda^{\text{ex}}$ and $\text{na}_{\mathbf{a}}(\mathbb{C})$ (resp., $\text{na}_{\mathbf{a}}^{\text{int}}(\mathbb{C})$ and $\text{na}_{\mathbf{a}}^{\text{ex}}(\mathbb{C})$) denote the number of vertices (resp., interior-vertices and exterior-vertices) v such that $\alpha(v) = \mathbf{a}$ in \mathbb{C} .
- A set $\Lambda_{\text{dg}}^{\text{int}} \subseteq \Lambda \times [1, 4]$ of chemical symbols and a set $\Gamma^{\text{int}} \subseteq \Gamma^{\text{int}}(D_\pi)$ of edge-configurations (μ, μ', m) with $\mu \leq \mu'$, where we require that the edge-configuration $\text{ec}(e)$ of an interior-edge e in \mathbb{C} belongs to Γ^{int} . We do not distinguish (μ, μ', m) and (μ', μ, m) .
- Define $\Gamma_{\text{ac}}^{\text{int}}$ to be the set of adjacency-configurations such that $\Gamma_{\text{ac}}^{\text{int}} := \{(\mathbf{a}, \mathbf{b}, m) \mid (\mathbf{a}\mathbf{d}, \mathbf{b}\mathbf{d}', m) \in \Gamma^{\text{int}}\}$. Let $\text{ac}_{\nu}^{\text{int}}(\mathbb{C}), \nu \in \Gamma_{\text{ac}}^{\text{int}}$ denote the number of interior-edges e such that $\text{ac}(e) = \nu$ in \mathbb{C} .
- Subsets $\Lambda^*(v) \subseteq \{\mathbf{a} \in \Lambda^{\text{int}} \mid \text{val}(\mathbf{a}) \geq 2\}, v \in V_{\mathbb{C}}$, we require that every chemical element $\alpha(v)$ assigned to a vertex $v \in V_{\mathbb{C}}$ in the seed graph belongs to $\Lambda^*(v)$.
- Lower and upper bound functions $\text{na}_{\text{LB}}, \text{na}_{\text{UB}} : \Lambda \rightarrow [1, n^*]$ and $\text{na}_{\text{LB}}^{\text{int}}, \text{na}_{\text{UB}}^{\text{int}} : \Lambda^{\text{int}} \rightarrow [1, n^*]$ on the number of interior-vertices v such that $\alpha(v) = \mathbf{a}$ in \mathbb{C} .
- Lower and upper bound functions $\text{ns}_{\text{LB}}^{\text{int}}, \text{ns}_{\text{UB}}^{\text{int}} : \Lambda_{\text{dg}}^{\text{int}} \rightarrow [1, n^*]$ on the number of interior-vertices v such that $\text{cs}(v) = \mu$ in \mathbb{C} .
- Lower and upper bound functions $\text{ac}_{\text{LB}}^{\text{int}}, \text{ac}_{\text{UB}}^{\text{int}} : \Gamma_{\text{ac}}^{\text{int}} \rightarrow \mathbb{Z}_+$ on the number of interior-edges e such that $\text{ac}(e) = \nu$ in \mathbb{C} .
- Lower and upper bound functions $\text{ec}_{\text{LB}}^{\text{int}}, \text{ec}_{\text{UB}}^{\text{int}} : \Gamma^{\text{int}} \rightarrow \mathbb{Z}_+$ on the number of interior-edges e such that $\text{ec}(e) = \gamma$ in \mathbb{C} .
- Lower and upper bound functions $\text{fc}_{\text{LB}}, \text{fc}_{\text{UB}} : \mathcal{F}^* \rightarrow [0, n^*]$ on the number of interior-vertices v such that $\mathbb{C}[v]$ is r-isomorphic to $\psi \in \mathcal{F}^*$ in \mathbb{C} .

- Lower and upper bound functions $\text{ac}_{\text{LB}}^{\text{lf}}, \text{ac}_{\text{UB}}^{\text{lf}} : \Gamma_{\text{ac}}^{\text{lf}} \rightarrow [0, n^*]$ on the number of leaf-edges uv in ac_{C} with adjacency-configuration ν .

We call a chemical graph \mathbb{C} that satisfies a chemical specification σ_{ce} a $(\sigma_{\text{int}}, \sigma_{\text{ce}})$ -extension of G_{C} , and denote by $\mathcal{G}(G_{\text{C}}, \sigma_{\text{int}}, \sigma_{\text{ce}})$ the set of all $(\sigma_{\text{int}}, \sigma_{\text{ce}})$ -extensions of G_{C} .

Table 8 shows an example of a chemical-specification σ_{ce} to the seed graph G_{C} in Figure 4.

Table 8: Example 2 of a chemical-specification σ_{ce} .

$n_{\text{LB}} = 30, n^* = 50.$																		
branch-parameter: $\rho = 2$																		
Each of sets $\mathcal{F}(v), v \in V_{\text{C}}$ and \mathcal{F}_E is set to be the set \mathcal{F} of chemical rooted trees ψ with $\text{ht}(\langle \psi \rangle) \leq \rho = 2$ in Figure 4(b).																		
$\Lambda = \{\text{H}, \text{C}, \text{N}, \text{O}, \text{S}_{(2)}, \text{S}_{(6)}, \text{P} = \text{P}_{(5)}\}$										$\Lambda_{\text{dg}}^{\text{int}} = \{\text{C2}, \text{C3}, \text{C4}, \text{N2}, \text{N3}, \text{O2}, \text{S}_{(2)}2, \text{S}_{(6)}3, \text{P4}\}$								
$\Gamma_{\text{ac}}^{\text{int}}$	$\nu_1 = (\text{C}, \text{C}, 1), \nu_2 = (\text{C}, \text{C}, 2), \nu_3 = (\text{C}, \text{N}, 1), \nu_4 = (\text{C}, \text{O}, 1), \nu_5 = (\text{C}, \text{S}_{(2)}, 1), \nu_6 = (\text{C}, \text{S}_{(6)}, 1), \nu_7 = (\text{C}, \text{P}, 1)$																	
Γ^{int}	$\gamma_1 = (\text{C2}, \text{C2}, 1), \gamma_2 = (\text{C2}, \text{C3}, 1), \gamma_3 = (\text{C2}, \text{C3}, 2), \gamma_4 = (\text{C2}, \text{C4}, 1), \gamma_5 = (\text{C3}, \text{C3}, 1), \gamma_6 = (\text{C3}, \text{C3}, 2), \gamma_7 = (\text{C3}, \text{C4}, 1), \gamma_8 = (\text{C2}, \text{N2}, 1), \gamma_9 = (\text{C3}, \text{N2}, 1), \gamma_{10} = (\text{C3}, \text{O2}, 1), \gamma_{11} = (\text{C2}, \text{C2}, 2), \gamma_{12} = (\text{C2}, \text{O2}, 1), \gamma_{13} = (\text{C3}, \text{N3}, 1), \gamma_{14} = (\text{C4}, \text{S}_{(2)}2, 2), \gamma_{15} = (\text{C2}, \text{S}_{(6)}3, 1), \gamma_{16} = (\text{C3}, \text{S}_{(6)}3, 1), \gamma_{17} = (\text{C2}, \text{P4}, 2), \gamma_{18} = (\text{C3}, \text{P4}, 1)$																	
$\Lambda^*(u_1) = \Lambda^*(u_8) = \{\text{C}, \text{N}\}, \Lambda^*(u_9) = \{\text{C}, \text{O}\}, \Lambda^*(u) = \{\text{C}\}, u \in V_{\text{C}} \setminus \{u_1, u_8, u_9\}$																		
	H	C	N	O	S ₍₂₎	S ₍₆₎	P		C	N	O	S ₍₂₎	S ₍₆₎	P				
$\text{na}_{\text{LB}}(\mathbf{a})$	40	27	1	1	0	0	0		$\text{na}_{\text{LB}}^{\text{int}}(\mathbf{a})$	9	1	0	0	0	0			
$\text{na}_{\text{UB}}(\mathbf{a})$	65	37	4	8	1	1	1		$\text{na}_{\text{UB}}^{\text{int}}(\mathbf{a})$	23	4	5	1	1	1			
	C2	C3	C4	N2	N3	O2	S ₍₂₎ 2	S ₍₆₎ 3	P4									
$\text{ns}_{\text{LB}}^{\text{int}}(\mu)$	3	5	0	0	0	0	0	0	0									
$\text{ns}_{\text{UB}}^{\text{int}}(\mu)$	8	15	2	2	3	5	1	1	1									
	ν_1	ν_2	ν_3	ν_4	ν_5	ν_6	ν_7											
$\text{ac}_{\text{LB}}^{\text{int}}(\nu)$	0	0	0	0	0	0	0											
$\text{ac}_{\text{UB}}^{\text{int}}(\nu)$	30	10	10	10	1	1	1											
	γ_1	γ_2	γ_3	γ_4	γ_5	γ_6	γ_7	γ_8	γ_9	γ_{10}	γ_{11}	γ_{12}	γ_{13}	γ_{14}	γ_{15}	γ_{16}	γ_{17}	γ_{18}
$\text{ec}_{\text{LB}}^{\text{int}}(\gamma)$	0	0	0	0	0	0	0	0	0	0	0	0	0	0	0	0	0	0
$\text{ec}_{\text{UB}}^{\text{int}}(\gamma)$	4	15	4	4	10	5	4	4	6	4	4	4	2	2	2	2	2	2
	$\psi \in \{\psi_i \mid i = 1, 6, 11\} \quad \psi \in \mathcal{F}^* \setminus \{\psi_i \mid i = 1, 6, 11\}$																	
$\text{fc}_{\text{LB}}(\psi)$	1			0														
$\text{fc}_{\text{UB}}(\psi)$	10			3														
	$\nu \in \{(\text{C}, \text{C}, 1), (\text{C}, \text{C}, 2)\} \quad \nu \in \Gamma_{\text{ac}}^{\text{lf}} \setminus \{(\text{C}, \text{C}, 1), (\text{C}, \text{C}, 2)\}$																	
$\text{ac}_{\text{LB}}^{\text{lf}}(\nu)$	0			0														
$\text{ac}_{\text{UB}}^{\text{lf}}(\nu)$	10			8														

Figure 2 illustrates an example \mathbb{C} of a $(\sigma_{\text{int}}, \sigma_{\text{ce}})$ -extension of G_{C} obtained from the σ_{int} -extension H^* in Figure 10 under the chemical-specification σ_{ce} in Table 8. Note that $r(\mathbb{C}) = r(H^*) = r(G_{\text{C}}) - 1 = 4$ holds since the edge in $E_{(0/1)}$ is discarded in H^* .

C Test Instances for Stages 4 and 5

We prepared the following instances (a)-(d) for conducting experiments of Stages 4 and 5 in Phase 2.

In Stages 4 and 5, we use three properties $\pi \in \{\text{OPTR}, \text{SFT}, \text{VIS}\}$ and define a set $\Lambda(\pi)$ of chemical elements as follows: $\Lambda(\text{OPTR}) = \Lambda_5 = \{\text{H}, \text{C}, \text{O}, \text{N}, \text{S}_{(2)}, \text{F}\}$ and $\Lambda(\text{SFT}) = \Lambda(\text{VIS}) = \Lambda_4 = \{\text{H}, \text{C}, \text{O}, \text{Si}_{(4)}\}$.

- (a) $I_a = (G_C, \sigma_{\text{int}}, \sigma_{\text{ce}})$: The instance introduced in Section B to explain the target specification. For each property π , we replace $\Lambda = \{\text{H}, \text{C}, \text{N}, \text{O}, \text{S}_{(2)}, \text{S}_{(6)}, \text{P}_{(5)}\}$ in Table 8 with $\Lambda(\pi) \cap \{\text{S}_{(2)}, \text{S}_{(6)}, \text{P}_{(5)}\}$ and remove from the σ_{ce} all chemical symbols, edge-configurations and fringe-configurations that cannot be constructed from the replaced element set (i.e., those containing a chemical element in $\{\text{S}_{(2)}, \text{S}_{(6)}, \text{P}_{(5)}\} \setminus \Lambda(\pi)$).
- (b) $I_b^i = (G_C^i, \sigma_{\text{int}}^i, \sigma_{\text{ce}}^i)$, $i = 1, 2, 3, 4$: An instance for inferring chemical graphs with rank at most 2. In the four instances I_b^i , $i = 1, 2, 3, 4$, the following specifications in $(\sigma_{\text{int}}, \sigma_{\text{ce}})$ are common.

Set $\Lambda := \Lambda(\pi)$ for a given property $\pi \in \{\text{OPTR}, \text{SFT}, \text{VIS}\}$, set $\Lambda_{\text{dg}}^{\text{int}}$ to be the set of all possible symbols in $\Lambda \times [1, 4]$ that appear in the data set D_π and set Γ^{int} to be the set of all edge-configurations that appear in the data set D_π . Set $\Lambda^*(v) := \Lambda$, $v \in V_C$.

The lower bounds ℓ_{LB} , bl_{LB} , ch_{LB} , $\text{bd}_{2,\text{LB}}$, $\text{bd}_{3,\text{LB}}$, na_{LB} , $\text{na}_{\text{LB}}^{\text{int}}$, $\text{ns}_{\text{LB}}^{\text{int}}$, $\text{ac}_{\text{LB}}^{\text{int}}$, $\text{ec}_{\text{LB}}^{\text{int}}$ and $\text{ac}_{\text{LB}}^{\text{lf}}$ are all set to be 0.

Set upper bounds $\text{na}_{\text{UB}}(\mathbf{a}) := n^*$, $\text{na} \in \{\text{H}, \text{C}\}$, $\text{na}_{\text{UB}}(\mathbf{a}) := 5$, $\text{na} \in \{\text{O}, \text{N}\}$, $\text{na}_{\text{UB}}(\mathbf{a}) := 2$, $\text{na} \in \Lambda \setminus \{\text{H}, \text{C}, \text{O}, \text{N}\}$. The other upper bounds ℓ_{UB} , bl_{UB} , ch_{UB} , $\text{bd}_{2,\text{UB}}$, $\text{bd}_{3,\text{UB}}$, $\text{na}_{\text{UB}}^{\text{int}}$, $\text{ns}_{\text{UB}}^{\text{int}}$, $\text{ac}_{\text{UB}}^{\text{int}}$, $\text{ec}_{\text{UB}}^{\text{int}}$ and $\text{ac}_{\text{UB}}^{\text{lf}}$ are all set to be an upper bound n^* on $n(G^*)$.

We specify n_{LB} as a parameter and set $n^* := n_{\text{LB}} + 10$, $n_{\text{LB}}^{\text{int}} := \lfloor (1/4)n_{\text{LB}} \rfloor$ and $n_{\text{LB}}^{\text{lf}} := \lfloor (3/4)n_{\text{LB}} \rfloor$.

For each property π , let $\mathcal{F}(D_\pi)$ denote the set of 2-fringe-trees in the compounds in D_π , and select a subset $\mathcal{F}_\pi^i \subseteq \mathcal{F}(D_\pi)$ with $|\mathcal{F}_\pi^i| = 45 - 5i$, $i \in [1, 5]$. For each instance I_b^i , set $\mathcal{F}_E := \mathcal{F}(v) := \mathcal{F}_\pi^i$, $v \in V_C$ and $\text{fc}_{\text{LB}}(\psi) := 0$, $\text{fc}_{\text{UB}}(\psi) := 10$, $\psi \in \mathcal{F}_\pi^i$.

Instance I_b^1 is given by the rank-1 seed graph G_C^1 in Figure 5(i) and Instances I_b^i , $i = 2, 3, 4$ are given by the rank-2 seed graph G_C^i , $i = 2, 3, 4$ in Figure 5(ii)-(iv).

- (i) For instance I_b^1 , select as a seed graph the monocyclic graph $G_C^1 = (V_C, E_C = E_{(\geq 2)} \cup E_{(\geq 1)})$ in Figure 5(i), where $V_C = \{u_1, u_2\}$, $E_{(\geq 2)} = \{a_1\}$ and $E_{(\geq 1)} = \{a_2\}$. We include a linear constraint $\ell(a_1) \leq \ell(a_2)$ and $5 \leq \ell(a_1) + \ell(a_2) \leq 15$ as part of the side constraint.
- (ii) For instance I_b^2 , select as a seed graph the graph $G_C^2 = (V_C, E_C = E_{(\geq 2)} \cup E_{(\geq 1)} \cup E_{(=1)})$ in Figure 5(ii), where $V_C = \{u_1, u_2, u_3, u_4\}$, $E_{(\geq 2)} = \{a_1, a_2\}$, $E_{(\geq 1)} = \{a_3\}$ and $E_{(=1)} = \{a_4, a_5\}$. We include a linear constraint $\ell(a_1) \leq \ell(a_2)$ and $\ell(a_1) + \ell(a_2) + \ell(a_3) \leq 15$.
- (iii) For instance I_b^3 , select as a seed graph the graph $G_C^3 = (V_C, E_C = E_{(\geq 2)} \cup E_{(\geq 1)} \cup E_{(=1)})$ in Figure 5(iii), where $V_C = \{u_1, u_2, u_3, u_4\}$, $E_{(\geq 2)} = \{a_1\}$, $E_{(\geq 1)} = \{a_2, a_3\}$ and $E_{(=1)} = \{a_4, a_5\}$. We include linear constraints $\ell(a_1) \leq \ell(a_2) + \ell(a_3)$, $\ell(a_2) \leq \ell(a_3)$ and $\ell(a_1) + \ell(a_2) + \ell(a_3) \leq 15$.

- (iv) For instance I_b^4 , select as a seed graph the graph $G_C^4 = (V_C, E_C = E_{(\geq 2)} \cup E_{(\geq 1)} \cup E_{(=1)})$ in Figure 5(iv), where $V_C = \{u_1, u_2, u_3, u_4\}$, $E_{(\geq 1)} = \{a_1, a_2, a_3\}$ and $E_{(=1)} = \{a_4, a_5\}$. We include linear constraints $\ell(a_2) \leq \ell(a_1) + 1$, $\ell(a_2) \leq \ell(a_3) + 1$, $\ell(a_1) \leq \ell(a_3)$ and $\ell(a_1) + \ell(a_2) + \ell(a_3) \leq 15$.

We define instances in (c) and (d) in order to find chemical graphs that have an intermediate structure of given two chemical cyclic graphs $G_A = (H_A = (V_A, E_A), \alpha_A, \beta_A)$ and $G_B = (H_B = (V_B, E_B), \alpha_B, \beta_B)$. Let Λ_A^{int} and $\Lambda_{\text{dg},A}^{\text{int}}$ denote the sets of chemical elements and chemical symbols of the interior-vertices in G_A , Γ_A^{int} denote the sets of edge-configurations of the interior-edges in G_A , and \mathcal{F}_A denote the set of 2-fringe-trees in G_A . Analogously define sets Λ_B^{int} , $\Lambda_{\text{dg},B}^{\text{int}}$, Γ_B^{int} and \mathcal{F}_B in G_B .

- (c) $I_c = (G_C, \sigma_{\text{int}}, \sigma_{\text{ce}})$: An instance aimed to infer a chemical graph G^\dagger such that the core of G^\dagger is equal to the core of G_A and the frequency of each edge-configuration in the non-core of G^\dagger is equal to that of G_B . We use chemical compounds CID 24822711 and CID 59170444 in Figure 6(a) and (b) for G_A and G_B , respectively.

Set a seed graph $G_C = (V_C, E_C = E_{(=1)})$ to be the core of G_A .

Set $\Lambda := \{\text{H}, \text{C}, \text{N}, \text{O}\}$, and set $\Lambda_{\text{dg}}^{\text{int}}$ to be the set of all possible chemical symbols in $\Lambda \times [1, 4]$.

Set $\Gamma^{\text{int}} := \Gamma_A^{\text{int}} \cup \Gamma_B^{\text{int}}$ and $\Lambda^*(v) := \{\alpha_A(v)\}$, $v \in V_C$.

Set $n_{\text{LB}}^{\text{int}} := \min\{n^{\text{int}}(G_A), n^{\text{int}}(G_B)\}$, $n_{\text{UB}}^{\text{int}} := \max\{n^{\text{int}}(G_A), n^{\text{int}}(G_B)\}$,

$n_{\text{LB}} := \min\{n(G_A), n(G_B)\} - 10 = 40$ and $n^* := \max\{n(G_A), n(G_B)\} + 5$.

Set lower bounds ℓ_{LB} , bl_{LB} , ch_{LB} , $\text{bd}_{2,\text{LB}}$, $\text{bd}_{3,\text{LB}}$, na_{LB} , $\text{na}_{\text{LB}}^{\text{int}}$, $\text{ns}_{\text{LB}}^{\text{int}}$, $\text{ac}_{\text{LB}}^{\text{int}}$ and $\text{ac}_{\text{LB}}^{\text{lf}}$ to be 0.

Set upper bounds $\text{na}_{\text{UB}}(\mathbf{a}) := n^*$, $\text{na} \in \{\text{H}, \text{C}\}$, $\text{na}_{\text{UB}}(\mathbf{a}) := 5$, $\text{na} \in \{\text{O}, \text{N}\}$, $\text{na}_{\text{UB}}(\mathbf{a}) := 2$, $\text{na} \in \Lambda \setminus \{\text{H}, \text{C}, \text{O}, \text{N}\}$ and set the other upper bounds ℓ_{UB} , bl_{UB} , ch_{UB} , $\text{bd}_{2,\text{UB}}$, $\text{bd}_{3,\text{UB}}$, $\text{na}_{\text{UB}}^{\text{int}}$, $\text{ns}_{\text{UB}}^{\text{int}}$, $\text{ac}_{\text{UB}}^{\text{int}}$ and $\text{ac}_{\text{UB}}^{\text{lf}}$ to be n^* .

Set $\text{ec}_{\text{LB}}^{\text{int}}(\gamma)$ to be the number of core-edges in G_A with $\gamma \in \Gamma^{\text{int}}$ and $\text{ec}_{\text{UB}}^{\text{int}}(\gamma)$ to be the number interior-edges in G_A and G_B with edge-configuration γ .

Let $\mathcal{F}_B^{(p)}$, $p \in [1, 2]$ denote the set of chemical rooted trees r-isomorphic p -fringe-trees in G_B ;

Set $\mathcal{F}_E := \mathcal{F}(v) := \mathcal{F}_B^{(1)} \cup \mathcal{F}_B^{(2)}$, $v \in V_C$ and $\text{fc}_{\text{LB}}(\psi) := 0$, $\text{fc}_{\text{UB}}(\psi) := 10$, $\psi \in \mathcal{F}_B^{(1)} \cup \mathcal{F}_B^{(2)}$.

- (d) $I_d = (G_C^1, \sigma_{\text{int}}, \sigma_{\text{ce}})$: An instance aimed to infer a chemical monocyclic graph G^\dagger such that the frequency vector of edge-configurations in G^\dagger is a vector obtained by merging those of G_A and G_B . We use chemical monocyclic compounds CID 10076784 and CID 44340250 in Figure 6(c) and (d) for G_A and G_B , respectively. Set a seed graph to be the monocyclic seed graph $G_C^1 = (V_C, E_C = E_{(\geq 2)} \cup E_{(\geq 1)})$ with $V_C = \{u_1, u_2\}$, $E_{(\geq 2)} = \{a_1\}$ and $E_{(\geq 1)} = \{a_2\}$ in Figure 5(i).

Set $\Lambda := \{\text{H}, \text{C}, \text{N}, \text{O}\}$, $\Lambda_{\text{dg}}^{\text{int}} := \Lambda_{\text{dg},A}^{\text{int}} \cup \Lambda_{\text{dg},B}^{\text{int}}$ and $\Gamma^{\text{int}} := \Gamma_A^{\text{int}} \cup \Gamma_B^{\text{int}}$.

Set $n_{\text{LB}}^{\text{int}} := \min\{n^{\text{int}}(G_A), n^{\text{int}}(G_B)\}$, $n_{\text{UB}}^{\text{int}} := \max\{n^{\text{int}}(G_A), n^{\text{int}}(G_B)\}$,

$n_{\text{LB}} := \min\{n(G_A), n(G_B)\} = 40$ and $n^* := \max\{n(G_A), n(G_B)\}$.

Set lower bounds ℓ_{LB} , bl_{LB} , ch_{LB} , $\text{bd}_{2,\text{LB}}$, $\text{bd}_{3,\text{LB}}$, na_{LB} , $\text{na}_{\text{LB}}^{\text{int}}$, $\text{ns}_{\text{LB}}^{\text{int}}$, $\text{ac}_{\text{LB}}^{\text{int}}$ and $\text{ac}_{\text{LB}}^{\text{lf}}$ to be 0.

Set upper bounds $\text{na}_{\text{UB}}(\mathbf{a}) := n^*$, $\text{na} \in \{\text{H}, \text{C}\}$, $\text{na}_{\text{UB}}(\mathbf{a}) := 5$, $\text{na} \in \{\text{O}, \text{N}\}$, $\text{na}_{\text{UB}}(\mathbf{a}) := 2$, $\text{na} \in \Lambda \setminus \{\text{H}, \text{C}, \text{O}, \text{N}\}$ and set the other upper bounds ℓ_{UB} , bl_{UB} , ch_{UB} , $\text{bd}_{2,\text{UB}}$, $\text{bd}_{3,\text{UB}}$, $\text{na}_{\text{UB}}^{\text{int}}$, $\text{ns}_{\text{UB}}^{\text{int}}$, $\text{ac}_{\text{UB}}^{\text{int}}$ and $\text{ac}_{\text{UB}}^{\text{lf}}$ to be n^* .

For each edge-configuration $\gamma \in \Gamma^{\text{int}}$, let $x_A^*(\gamma^{\text{int}})$ (resp., $x_B^*(\gamma^{\text{int}})$) denote the number of

interior-edges with γ in G_A (resp., G_B), $\gamma \in \Gamma^{\text{int}}$ and set

$$x_{\min}^*(\gamma) := \min\{x_A^*(\gamma), x_B^*(\gamma)\}, \quad x_{\max}^*(\gamma) := \max\{x_A^*(\gamma), x_B^*(\gamma)\},$$

$$\text{ec}_{\text{LB}}^{\text{int}}(\gamma) := \lfloor (3/4)x_{\min}^*(\gamma) + (1/4)x_{\max}^*(\gamma) \rfloor \text{ and}$$

$$\text{ec}_{\text{UB}}^{\text{int}}(\gamma) := \lceil (1/4)x_{\min}^*(\gamma) + (3/4)x_{\max}^*(\gamma) \rceil.$$

Set $\mathcal{F}_E := \mathcal{F}(v) := \mathcal{F}_A \cup \mathcal{F}_B$, $v \in V_C$ and $\text{fc}_{\text{LB}}(\psi) := 0$, $\text{fc}_{\text{UB}}(\psi) := 10$, $\psi \in \mathcal{F}_A \cup \mathcal{F}_B$.

We include a linear constraint $\ell(a_1) \leq \ell(a_2)$ and $5 \leq \ell(a_1) + \ell(a_2) \leq 15$ as part of the side constraint.